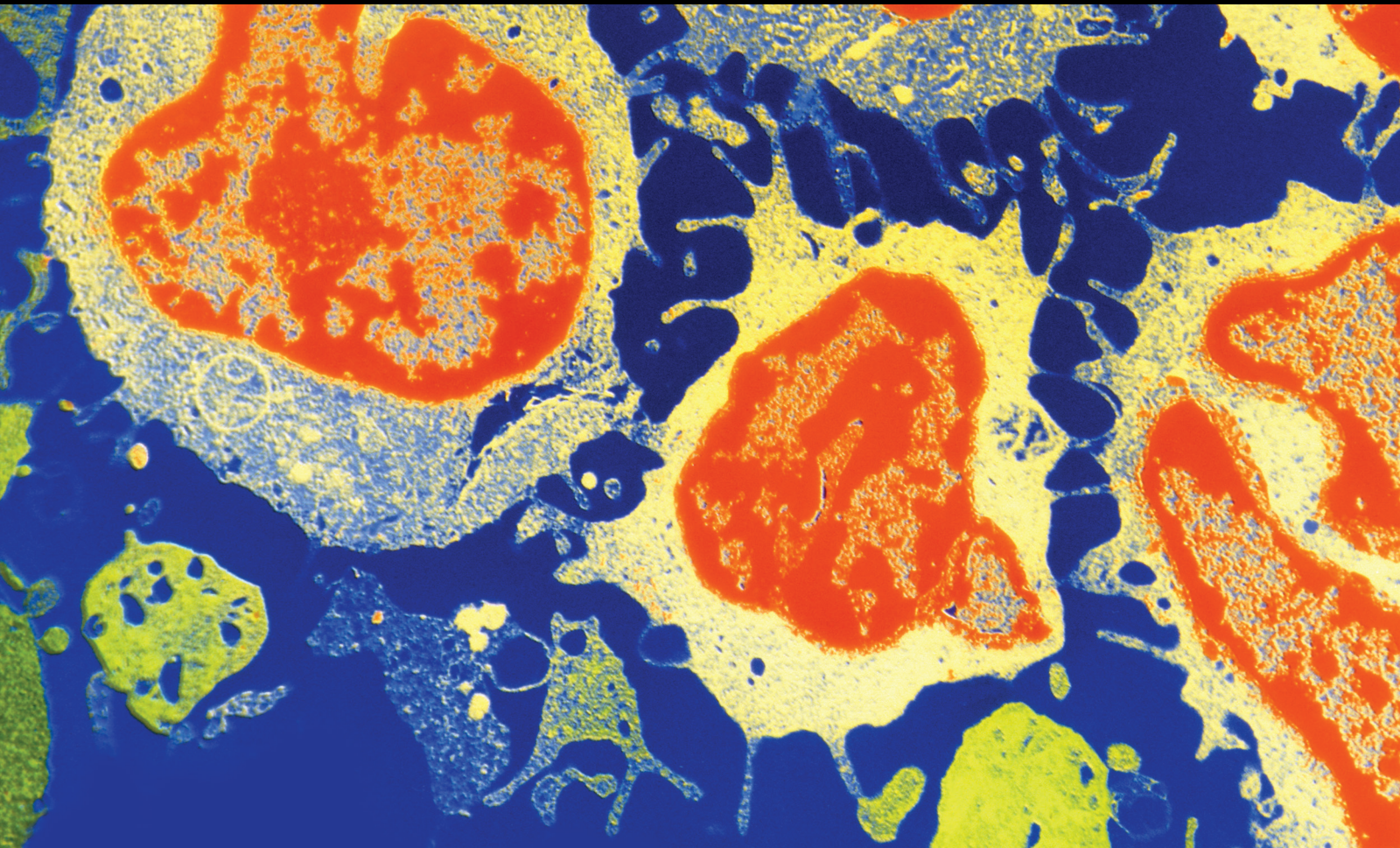


Radiotherapy: Innovative Techniques, Radiosensitizers, Radioprotectors, Multi-modality Treatment Strategies, Prognostic Biomarkers, and Microenvironment Factors

Lead Guest Editor: Ming-Yii Huang

Guest Editors: Chih-Hung Chuang, Woong Soup Koom, and Ya-Ju Hsieh





**Radiotherapy: Innovative Techniques,
Radiosensitizers, Radioprotectors, Multi-
modality Treatment Strategies, Prognostic
Biomarkers, and Microenvironment Factors**

Journal of Oncology

**Radiotherapy: Innovative Techniques,
Radiosensitizers, Radioprotectors,
Multi-modality Treatment Strategies,
Prognostic Biomarkers, and
Microenvironment Factors**

Lead Guest Editor: Ming-Yii Huang

Guest Editors: Chih-Hung Chuang, Woong Soup
Koom, and Ya-Ju Hsieh



Copyright © 2023 Hindawi Limited. All rights reserved.

This is a special issue published in "Journal of Oncology" All articles are open access articles distributed under the Creative Commons Attribution License, which permits unrestricted use, distribution, and reproduction in any medium, provided the original work is properly cited.

Chief Editor

Bruno Vincenzi, Italy

Academic Editors

Thomas E. Adrian, United Arab Emirates

Ruhai Bai , China

Jiaolin Bao, China

Rossana Berardi, Italy

Benedetta Bussolati, Italy

Sumanta Chatterjee, USA

Thomas R. Chauncey, USA

Gagan Chhabra, USA

Francesca De Felice , Italy

Giuseppe Di Lorenzo, Italy

Xiangya Ding , China

Peixin Dong , Japan

Xingrong Du, China

Elizabeth R. Dudnik , Israel

Pierfrancesco Franco , Italy

Ferdinand Frauscher , Austria

Rohit Gundamaraju, USA

Han Han , USA

Jitti Hanprasertpong , Thailand

Yongzhong Hou , China

Wan-Ming Hu , China

Jialiang Hui, China

Akira Iyoda , Japan

Reza Izadpanah , USA

Kaiser Jamil , India

Shuang-zheng Jia , China

Ozkan Kanat , Turkey

Zhijia Kang , USA

Pashtoon M. Kasi , USA

Jorg Kleeff, United Kingdom

Jayaprakash Kolla, Czech Republic

Goo Lee , USA

Peter F. Lenehan, USA

Da Li , China

Rui Liao , China

Rengyun Liu , China

Alexander V. Louie, Canada

Weiren Luo , China

Cristina Magi-Galluzzi , USA

Kanjoormana A. Manu, Singapore

Riccardo Masetti , Italy

Ian E. McCutcheon , USA

Zubing Mei, China

Giuseppe Maria Milano , Italy

Nabiha Missaoui , Tunisia

Shinji Miwa , Japan

Sakthivel Muniyan , USA

Magesh Muthu , USA

Nandakumar Natarajan , USA

P. Neven, Belgium

Patrick Neven, Belgium

Marco Noventa, Italy

Liren Qian , China

Shuanglin Qin , China

Dongfeng Qu , USA

Amir Radfar , USA

Antonio Raffone , Italy

Achuthan Chathrattil Raghavamenon, India

Faisal Raza, China

Giandomenico Roviello , Italy

Subhadeep Roy , India

Prasannakumar Santhekadur , India

Chandra K. Singh , USA

Yingming Sun , China

Mohammad Tarique , USA

Federica Tomao , Italy

Vincenzo Tombolini , Italy

Maria S. Tretiakova, USA

Abhishek Tyagi , USA

Satoshi Wada , Japan

Chen Wang, China

Xiaosheng Wang , China

Guangzhen Wu , China

Haigang Wu , China

Yuan Seng Wu , Malaysia

Yingkun Xu , China

WU Xue-liang , China

ZENG JIE YE , China

Guan-Jun Yang , China

Junmin Zhang , China

Dan Zhao , USA

Dali Zheng , China

Contents

IDO1 Activity Predicts Lung Toxicity in Patients with Unresectable Stage III NSCLC and Chemoradiotherapy

Linfang Wu , Yibo Gao , Daquan Wang, Yanhua Chen, Mingmin Qian, Xin Xu, Tao Zhang, Nan Bi , and Luhua Wang 

Research Article (8 pages), Article ID 3591758, Volume 2023 (2023)

Long-Term Follow-Up Results of Adjuvant Intensity-Modulated Radiotherapy with Concurrent Paclitaxel and Cisplatin in High-Risk Endometrial Cancer Patients

Pei Shu , Xin Wang , Ganlu Ouyang , Jitao Zhou , Yaqin Zhao , Fang Wang , Zhiping Li , and Yali Shen 

Research Article (8 pages), Article ID 4621240, Volume 2022 (2022)

miR-3059-3p Regulates Glioblastoma Multiforme Radiosensitivity Enhancement through the Homologous Recombination Pathway of DNA Repair

Yu-Wen Cheng, Chien-Ju Lin, Shih-Hsun Kuo, Ann-Shung Lieu, Chee-Yin Chai, Hung-Pei Tsai , and Aij-Lie Kwan 

Research Article (10 pages), Article ID 7250278, Volume 2022 (2022)

Comparable Clinical Outcome Using Small or Large Gross Tumor Volume-to-Clinical Target Volume Margin Expansion in Neoadjuvant Chemoradiotherapy for Esophageal Squamous Cell Carcinoma

Tae Hoon Lee , Hak Jae Kim , Byoung Hyuck Kim , Chang Hyun Kang , Bhumsuk Keam , Hyeon Jong Moon , Yong Won Seong , and Suzy Kim 

Research Article (10 pages), Article ID 5635071, Volume 2022 (2022)

Research Article

IDO1 Activity Predicts Lung Toxicity in Patients with Unresectable Stage III NSCLC and Chemoradiotherapy

Linfang Wu ¹, Yibo Gao ^{2,3,4,5}, Daquan Wang,¹ Yanhua Chen,⁶ Mingmin Qian,⁶ Xin Xu,¹ Tao Zhang,¹ Nan Bi ¹, and Luhua Wang ^{1,7}

¹Department of Radiation Oncology, National Cancer Center/National Clinical Research Center for Cancer/Cancer Hospital, Chinese Academy of Medical Sciences and Peking Union Medical College, Beijing 100021, China

²Central Laboratory, National Cancer Center/National Clinical Research Center for Cancer/Cancer Hospital and Shenzhen Hospital, Chinese Academy of Medical Sciences and Peking Union Medical College, Shenzhen 518116, China

³Laboratory of Translational Medicine, National Cancer Center/National Clinical Research Center for Cancer/Cancer Hospital, Chinese Academy of Medical Sciences and Peking Union Medical College, Beijing 100021, China

⁴State Key Laboratory of Molecular Oncology, National Cancer Center/National Clinical Research Center for Cancer/Cancer Hospital, Chinese Academy of Medical Sciences and Peking Union Medical College, Beijing 100021, China

⁵Department of Thoracic Surgery, National Cancer Center/National Clinical Research Center for Cancer/Cancer Hospital, Chinese Academy of Medical Sciences and Peking Union Medical College, Beijing 100021, China

⁶Key Laboratory of Mass Spectrometry Imaging and Metabolomics, Minzu University of China, National Ethnic Affairs Commission, Beijing 100081, China

⁷Department of Radiation Oncology, National Cancer Center/National Clinical Research Center for Cancer/Cancer Hospital and Shenzhen Hospital, Chinese Academy of Medical Sciences and Peking Union Medical College, Shenzhen 518116, China

Correspondence should be addressed to Nan Bi; binan_email@163.com and Luhua Wang; wlhqwq@yahoo.com

Received 6 September 2022; Revised 27 October 2022; Accepted 25 November 2022; Published 14 February 2023

Academic Editor: Ya Ju Hsieh

Copyright © 2023 Linfang Wu et al. This is an open access article distributed under the Creative Commons Attribution License, which permits unrestricted use, distribution, and reproduction in any medium, provided the original work is properly cited.

Objectives. Indoleamine 2,3-dioxygenase 1 (IDO1) acts as the key rate-limiting enzyme that converts tryptophan (Trp) to kynurenine (Kyn). Its activity was primarily induced by interferon- γ (IFN- γ), which was reported to play a role in the development of acute radiation-induced pneumonitis. In this study, we aimed to investigate the correlation between IDO1 activity and radiation-induced lung toxicity (RILT) in stage III nonsmall cell lung cancer (NSCLC) patients who were treated with chemoradiotherapy (CRT). **Materials and Methods.** Systemic IDO1 activity was reflected by Kyn:Trp ratio. Plasma levels of Kyn and Trp in 113 stage III NSCLC patients were measured by high-performance liquid chromatography (HPLC) before the initiation of radiotherapy. Dynamic change of IDO1 activity was followed in 23 patients before, during, and after radiotherapy. We also used RNA sequencing (RNA-seq) data from the Cancer Genome Atlas Program (TCGA) database and performed gene set enrichment analysis (GSEA) to explore how IDO1 was involved in the development of RILT. **Results.** 9.7% (11/113) of the whole group developed G3+ (greater than or equal to Grade 3) RILT. Preradiation IDO1 activity was significantly higher in patients who developed G3+ RILT than in nonG3+ RILT patients. ($P = 0.029$, AUC = 0.70). Univariate and multivariate analyses showed that high IDO1 activity was independently associated with the risk of G3+ RILT ($P = 0.034$). A predictive model combining both IDO1 activity and FEV1 was established for severe RILT and displayed a moderate predictive value (AUC = 0.83, $P < 0.001$). The incidence of G3+ RILT was 2.6% (1/38) in patients with an IDO activity ≤ 0.069 and FEV1 $> 59.4\%$, and 50.0% (6/12) in those with an IDO activity > 0.069 and FEV1 $\leq 59.4\%$. Of 23 patients with dynamic tracking, the IDO1 activity of postirradiation was significantly lower than midirradiation ($P = 0.021$), though no significant differences among the three time points were observed

($P = 0.070$). Bioinformatic analysis using RNA-seq data from 1014 NSCLC patients revealed that IDO mainly functioned in the inflammatory response instead of the late fibrosis process in NSCLC patients. **Conclusion.** High baseline IDO1 activity combined with unfavorable baseline FEV1 was predictive of severe RILT in unresectable stage III NSCLC patients. IDO1 might play a role in the acute inflammatory response. Finding effective interventions to alleviate RILT using IDO inhibitors is warranted in the future.

1. Introduction

Lung cancer is one of the most lethal cancer types in China, with 85% of the patients being nonsmall cell lung cancer (NSCLC) [1, 2]. Definitive chemoradiotherapy (CRT) with consolidated immunotherapy is the standard of care for unresectable stage NSCLC patients [3]. Thoracic radiation therapy (RT) plays a pivotal role in treating NSCLC, whereas causing radiation-induced lung toxicity (RILT). With the symptoms of cough, dyspnea, fever, and fibrotic changes on computed tomography (CT), RILT can impair the lung function of patients, leading to respiratory failure and even treatment-related mortality [4, 5]. G3+ (greater than or equal to Grade 3) RILT or severe RILT happens in about 10% of patients and has raised increasing attention due to its high lethality [6, 7]. Thus, it is of great significance to predict RILT, particularly severe RILT, in advance of radiation. Despite emerging attempts to build predictive models, there is still no effective model available for RILT in clinical practice [6, 8–11].

Indoleamine 2,3-dioxygenase 1 (IDO1) is the key rate-limiting enzyme in the tryptophan (Trp) metabolic reaction, serving as the most active enzyme that converts the essential amino acid L-Trp into L-kynurenine (Kyn) [12]. IDO1 is highly and constitutively expressed in NSCLC patients and acts as an immune checkpoint induced by potent mediators such as interferon- γ (IFN- γ), transforming growth factor- β (TGF- β), and other proinflammatory signals in the tumor microenvironment [13–16]. A study performed in colorectal cancer cell lines and animal models has shown that IDO1 blockade protected the normal small intestinal epithelium from radiation toxicity and accelerated recovery from radiation-induced side effects [17]. Even though the mechanism was not specifically depicted in the study, it is noted that a correlation might exist between IDO status and radiation-induced toxicity.

There has been limited study relating to IDO's role in the mechanism of RILT. A review on the crosstalk among signaling pathways in RILT and immunotherapy-related lung injury (IRLI) demonstrated that cell damage caused by radiotherapy contributed to the release of numerous cytokines, including IFN- γ , TGF- β , and interleukin (IL)-6, which consequently induced lung injury [18]. Therefore, cytokines predictive of RILT were widely explored. Aso et al. reported that pretreatment IFN- γ was overexpressed in patients with severe radiation pneumonitis (RP) [19]. Another research demonstrated that IFN- γ serum levels 3 weeks after RT initiation could identify NSCLC patients predisposed to severe RP [20]. Despite the small sample size of the two studies, IFN- γ could be identified as an indicator

for acute RP [18, 21]. TGF- β is another classical candidate; however, some studies failed to find the independent predictive value of TGF- β 1 for RILT, mainly because of improper sample handling, indicating it is a less practical biomarker for RILT in the clinical setting [22, 23]. Other cytokines related to lung injury, such as tumor necrosis factor (TNF), interleukin (IL)-1, and IL-6, were not reliable either because some of the elevations happened only after RT [8]. Therefore, it would be preferable to determine a novel and stable biomarker indicating the risk of RILT before the initiation of RT in a larger cohort. IDO1 was broadly activated through the canonical IFN- γ -IDO axis, and IDO1 can function as a signaling molecule in the regulatory circuit in response to TGF- β -driven homeostatic tolerance [24, 25]. Therefore, the upregulated activity of IDO1 by proinflammatory cytokines might indicate a higher risk of developing RILT. The Kyn:Trp ratio in serum of lung cancer patients is widely used to reflect the activity of IDO1 with minimal invasiveness [14]. We measured the baseline and dynamic levels of Kyn and Trp in CRT-received NSCLC patients to explore the association between IDO1 activity and RILT. We also performed bioinformatic analyses to elucidate how IDO1 participated in the phase of RILT development.

2. Materials and Methods

2.1. Study Population and Treatment. Eligible subjects include patients pathologically diagnosed with unresectable stage III NSCLC as per the American Joint Committee on Cancer (AJCC) 8th edition cancer staging manual between January 2013 and December 2017 at our institution. All patients underwent radiotherapy with or without concurrent or sequential chemotherapy. Radiation was delivered using intensity-modulated radiotherapy (IMRT), with 6-MV X-ray implemented. The median total dose is 60 Gy (28–67 Gy) in 30 (13–33) fractions. The chemotherapy regimen mainly consisted of etoposide/cisplatin and paclitaxel/carboplatin. The study was approved by the institutional review board of the National Cancer Center, Chinese Academy of Medical Sciences, and Peking Union Medical College (IRB No. NCC-000302). All patients provided written informed consent before therapy.

2.2. Toxicity Evaluation. RILT, including radiation pneumonitis and clinical fibrosis, is a diagnosis of exclusion. Chest computed tomography (CT) manifestations, physical examination, and clinical symptoms were taken into account when evaluating and grading RILT according to the

Common Terminology Criteria for Adverse Events (CTCAE), version 4.0. Pneumonitis caused by infectious or cardiopulmonary diseases was excluded. During CRT or follow-up period, enhanced chest CT scans were routinely carried out to evaluate lung toxicity. Respiratory symptoms of patients were also inquired about routinely. Patients who presented with cough, dyspnea, or any other respiratory symptoms would get extra CT scans and laboratory tests depending on the senior clinician's decisions.

2.3. Sample Collection and Measurement of Trp and Kyn. Plasma samples were prospectively collected one week before RT (pre-RT), four weeks during RT (mid-RT), and within one week after RT (post-RT). A total of 113 patients had pre-RT samples, and 23 of them had dynamic tracing at the three-time points. Liquid chromatography-tandem mass spectrometry (LC-MS/MS) was performed to quantify the plasma Trp and Kyn. The plasma samples were stored at -80°C until analysis. Eighty microliters of plasma samples were vortex mixed with $240\ \mu\text{L}$ of frozen acetonitrile and $8\ \mu\text{L}$ of internal standard solution and centrifuged at 10,000 rpm for 5 min. After centrifugation, the upper layer was concentrated and redissolved in $80\ \mu\text{L}$ of 2% acetonitrile solution. After filtering through a 96-well plate, five microliters of the solution was injected for LC-MS/MS analysis. The LC-MS/MS was performed on high-performance liquid chromatography coupled to a tandem mass spectrometry system (QTRAP 6500, AB SCIEX, USA) with an electrospray ionization (ESI) source and controlled by the Analyst 1.6.1 Software. The chromatographic separation was achieved on a reversed-phase Waters HSS T3 column ($2.1 \times 100\ \text{mm}$, $1.8\ \mu\text{m}$), and the column temperature was maintained at 35°C . It was composed of water containing 0.1% formic acid (A) and 100% acetonitrile (B) using an elution gradient. The flow rate is $250\ \mu\text{L}/\text{min}$. Data were acquired in the positive ion mode of the multiple reaction monitoring (MRM) scans. Raw data were first processed with MultiQuant 2.2 software (AB SCIEX, USA) and then calibrated using the Norm ISWSVR program in Python 3.6.

2.4. Follow-up and Statistical Analyses. The median follow-up time was 63.0 months. Patients were evaluated weekly during RT, one month after RT, and then every 3 months for 2 years and every 6 months for another 3 years. Blood tests, chest and abdomen CT scans (enhanced required if without contradictions), bone scans, and brain magnetic resonance imaging (MRI) were routinely performed during the follow-up. Patients and treatment characteristics, including age, gender, Eastern Cooperative Oncology Group Performance Status Scale (ECOG-PS), smoking status, pulmonary function tests (PETs), histology, clinical stage, tumor location, dose-volume parameters such as mean lung dose (MLD) and the percentage of lung volume minus gross tumor volume receiving over 5 Gy (V5) or over 20 Gy (V20), were retrieved in the electronic medical record.

The primary endpoint was G3 + RILT. Mann-Whitney U test, Kruskal-Wallis test, paired T-test, and Friedman's test were adopted for general data comparison between unpaired

TABLE 1: Patient baseline characteristics.

Variables	No. of patients	Data
Sex (male/female)	113	98/15
Age	113	62 (35–80)
ECOG-PS (<2 vs. \geq 2)	113	63/50
Smoking history (yes/no)	113	92/21
Clinical stage (IIIA/IIIB/IIIC)	113	26/64/23
Histology (SCC vs. non-SCC)	113	76/37
Location (lower vs. other)	113	34/79
Therapy (CCRT/SCRT/RT alone)	113	54/43/16
FVC%	96	74.00 (36.30–109.60)
FEV1%	96	73.20 (18.70–113.50)
DLCO%	96	63.70 (12.10–122.00)
Radiation dose (Gy)	113	60.00 (27.90–67.00)
V5%	113	55.05 (31.65–88.49)
V20%	113	23.69 (12.00–46.80)
MLD (Gy)	113	14.36 (7.84–22.01)
Tryptophan ($\mu\text{mol}/\text{L}$)	113	26.70 (11.44–40.03)
Kynurenine ($\mu\text{mol}/\text{L}$)	113	1.79 (0.56–5.03)
Kyn/Trp ratio ($\times 100$)	113	6.87 (2.58–19.82)

All continuous variables in the dataset present with median and range values. ECOG-PS, eastern cooperative oncology group-performance status; SCC, squamous cell carcinoma; CCRT, concurrent chemoradiotherapy; SCRT, sequential chemoradiotherapy; RT, radiotherapy; FVC, forced vital capacity; DLCO diffusing capacity for carbon monoxide; FEV1, forced expiratory volume in the first second; V5, percentage of lung volume minus gross tumor volume receiving $>5\ \text{Gy}$; V20, the percentage of lung volume minus gross tumor volume receiving $>20\ \text{Gy}$; MLD, mean lung dose; Kyn/Trp ratio, an indicator of IDO activity.

or paired groups. The area under the curve (AUC) determined by receiver operating characteristic (ROC) analysis was employed to evaluate the predictive ability of covariates for G3 + RILT. Logistic regression models were used for univariate and multivariate analyses to identify the risk factor (s) of G3 + RILT, and median values were chosen to be the cutoff points for all continuous variables. RNA-sequencing expression profiles and corresponding clinical information for NSCLC were downloaded from the TCGA dataset (<https://portal.gdc.com>). R software GSVA package was used to analyze, choosing parameter as `method = "ssgsea"` [26]. The correlation between gene and pathway scores was analyzed by Spearman correlation. All analysis methods and R packages were implemented by R version 4.0.3. All *P* values are two-sided, and $P < 0.05$ was considered to indicate statistical significance.

3. Results

3.1. Patient Characteristics. As it is shown in Table 1, 113 NSCLC patients with qualified plasma samples were enrolled in the study. Of these, 96 (85.0%) received pulmonary function tests (PETs), and 111 (98.2%) had complete dosimetric parameters retrieved. The median age of the

population was 62 years old (range, 35–80), and most (86.7%) were males. Only 16 (14.2%) of the group underwent radiotherapy alone, and 54 (47.8%) received concurrent chemoradiotherapy (CCRT). The median radiation dose was 60 Gy, with the majority (94.7%) dosed over 50 Gy.

3.2. Incidence of RILT. Among the 113 patients, 23.0% (26/113) developed G2 + RILT, 9.7% (11/113) had G3 + RILT, with two patients who died from fatal lung toxicity. No patients experienced Grade 4 RILT. Patients with severe lung toxicity were all identified within one year since their first irradiation during the follow-up.

3.3. Correlation between IDO Activity and RILT. The median Kyn:Trp ratio of the whole group was 0.07 before radiotherapy. Kyn:Trp ratio indicates the level of IDO activity as previously described. The median preRT Kyn:Trp ratio was 0.09 in patients with G3 + RILT, which was significantly higher than in the non-G3 + population (0.09 vs. 0.06, $P = 0.029$, Figure 1).

The analyses of risk factors for G3 + RILT are shown in Table 2. Continuous covariates including forced expiratory volume in the first second (FEV1), forced vital capacity (FVC), diffusing capacity for carbon monoxide (DLCO), V5, V20, MLD, Trp, Kyn, and Kyn:Trp ratio were dichotomized using the median value as the cutoff point. Three risk factors with a P value less than 0.1 were identified in the univariate analysis and then included in the multivariate analysis. The result showed that the preRT Kyn:Trp ratio was significantly correlated with the rate of G3 + RILT (OR: 10.21; 95% confidence interval [CI]: 1.20–87.30; $P = 0.034$). High baseline FEV1 tended to be a protective factor for lung toxicity, although no significance was noted (OR: 0.21; 95% CI: 0.40–1.13; $P = 0.070$).

Then ROC analysis was performed on 96 patients to explore the combined predictive value of IDO activity and PETs parameters for G3 + RILT. Three ROC curves are shown in Figure 2. The combination of IDO activity and FEV1 displayed the best predictive ability (AUC = 0.83, $P < 0.001$), as compared with IDO and FVC (AUC = 0.79, $P = 0.002$), or IDO activity alone (AUC = 0.68, $P = 0.058$). By using ROC analysis, the optimal cutoff points for FEV1 and IDO activity were calculated as 59.4% and 0.069, respectively. The incidence of G3 + RILT was 2.6% (1/38) in patients with an IDO activity ≤ 0.069 and FEV1 $> 59.4\%$, and 50.0% (6/12) in those with an IDO activity > 0.069 and FEV1 $\leq 59.4\%$.

3.4. Dynamics of IDO Activity. IDO activity was dynamically monitored in 23 patients during RT. The median Kyn:Trp ratio ($\times 100$) was 6.22 before RT, 7.02 at four weeks after RT, and 4.86 after RT, respectively. According to the Friedman test, the IDO activity was not significantly different among the three time points ($P = 0.07$). Paired comparisons are shown in Figure 3. IDO levels descended prominently at the end of RT as compared to mid-RT levels ($P = 0.021$) but remained relatively stable in the first four weeks of RT.

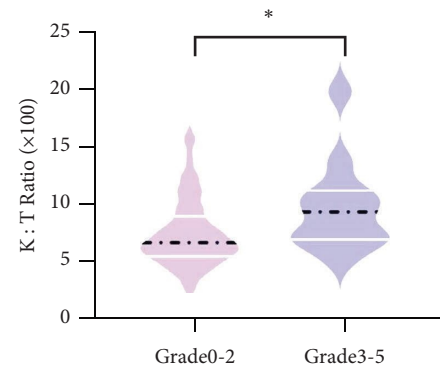


FIGURE 1: The comparison of preradiation IDO activity between patients with G3 + RILT and non G3 + RILT ($P = 0.029$). K:T ratio is an indicator of IDO activity.

3.5. Correlations between IDO1 and Six Pathways. To explore how IDO1 took part in the development of RILT, we conducted a correlation analysis between IDO1 and six common gene pathways involved in pulmonary fibrosis and inflammation based on the TCGA database. The six pathways related to genes were involved in extracellular matrix (ECM), collagen formation, degradation of ECM, TGF- β , tumor inflammation, and inflammatory response. As it is shown in Figure 4, IDO1 expression was significantly correlated with the inflammatory response in NSCLC patients (Spearman correlation score = 0.67, 95% CI: 0.63–0.70, $P = 1.78e-131$), while the correlation scores of the other five pathways were too low to indicate any correlation. By the fact that all severe RILT in our cohort occurred within six months from the start of RT, during which the acute or early phase of RILT usually happened, we assume that IDO1 was primarily correlated with inflammatory response rather than fibrosis [27].

4. Discussion

Data from our study demonstrate that the combination of pre-RT IDO activity and FEV1 can be used to construct a predictive model for severe RILT. To our knowledge, this is the first study in the literature that associates this novel metabolomics biomarker with radiation-induced toxicity in lung cancer patients. We also use a bioinformatic tool to establish a correlation between IDO1 and acute inflammatory response and thus enlighten thinking in the usage of IDO inhibitors to alleviate RILT. More importantly, both IDO1 activity and FEV1 were obtained relatively easily before the initiation of radiation, indicating that the model can serve as a promising and convenient tool for prescribing individualized RT plans in clinical practice.

IDO1 could be used as a blood biomarker for G3 + RILT. The rationale might be that IDO1 was primarily induced by IFN- γ and served as a responder to TGF- β , both of which were involved in inducing lung injury and predictive of RILT. Therefore, high levels of pre-RT IDO1 might predispose patients to acute RP. This hypothesis was per the analysis results from the TCGA database. It is worth noting that even though we tracked 23 patients dynamically and

TABLE 2: Univariate and multivariate analyses of severe RILT (grade ≥ 3) in patients with stage III non-small-cell lung cancer treated with chemoradiotherapy ($N=113$).

Variable	Univariate analysis			Multivariate analysis		
	Odds ratio	95% CI	<i>p</i> -value	Odds ratio	95% CI	<i>p</i> -value
Age (≥ 62 vs. <62)	3.52	0.88–14.02	0.075	2.57	0.57–11.56	0.218
ECOG-PS (2 vs. 1)	1.58	0.45–5.52	0.472			
Tumor location (lower lobe vs. nonlower lobe)	1.23	0.44–3.47	0.691			
Histology (squamous vs. nonsquamous)	0.43	0.09–2.08	0.291			
%FVC ($n=96$) ($\geq 74.0\%$ vs. $<74.0\%$)	0.41	0.10–1.69	0.216			
%DLCO ($n=96$) ($\geq 63.7\%$ vs. $<63.7\%$)	0.64	0.17–2.42	0.507			
%FEV1 ($n=96$) ($\geq 73.2\%$ vs. $<73.2\%$)	0.22	0.04–1.08	0.063	0.21	0.40–1.13	0.070
Concurrent radiotherapy (yes vs. no)	1.75	0.48–6.35	0.395			
V5% ($\geq 55.0\%$ vs. $<55.0\%$)	1.82	0.50–6.60	0.362			
V20% ($\geq 23.9\%$ vs. $<23.9\%$)	0.80	0.23–2.79	0.728			
MLD (Gy) (≥ 14.4 vs. <14.4)	0.80	0.23–2.79	0.728			
Tryptophan ($\mu\text{mol/L}$) (≥ 26.7 vs. <26.7)	0.35	0.09–1.38	0.133			
Kynurenine ($\mu\text{mol/L}$) (≥ 1.80 vs. <1.80)	1.25	0.39–4.35	0.728			
Kyn/Trp ratio ($\times 100$) (≥ 6.9 vs. <6.9)	11.3	1.39–91.14	0.023	10.21	1.20–87.30	0.034

Continuous variables were dichotomized using the median as the cutoff point. ECOG-PS, eastern cooperative oncology group-performance status; SCC, squamous cell carcinoma; FVC, forced vital capacity; DLCO, diffusing capacity for carbon monoxide; FEV1, forced expiratory volume in the first second; V5, the percentage of lung volume minus gross tumor volume receiving >5 Gy; V20, the percentage of lung volume minus gross tumor volume receiving >20 Gy; MLD, mean lung dose; Kyn/Trp ratio, an indicator of IDO activity.

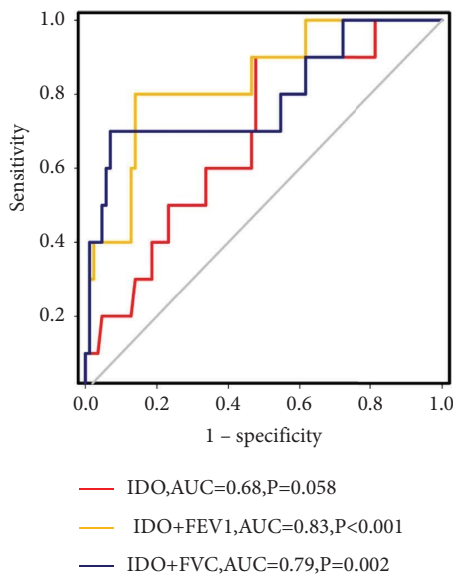


FIGURE 2: The combination of IDO activity with FEV1 or FVC showed improvement in the prediction of G3 + RILT as compared with IDO activity alone. Abbreviations: FVC, forced vital capacity; FEV1, forced expiratory volume in the first second.

observed no significant variation in IDO1 activity during RT, we could not assess whether the levels of IDO activity at mid-RT or post-RT were predictive of RILT due to the small sample size. Further research is needed to validate our results in a larger population, and the internal mechanisms remain to be explored.

Our study might enlighten a more extensive usage of IDO1 inhibitors to reduce radiation-induced toxicity in the future. Much attention of IDO1 in RT was its role as a targetable immune mediator, without mentioning toxicity. Research has shown that IDO1 levels were influenced

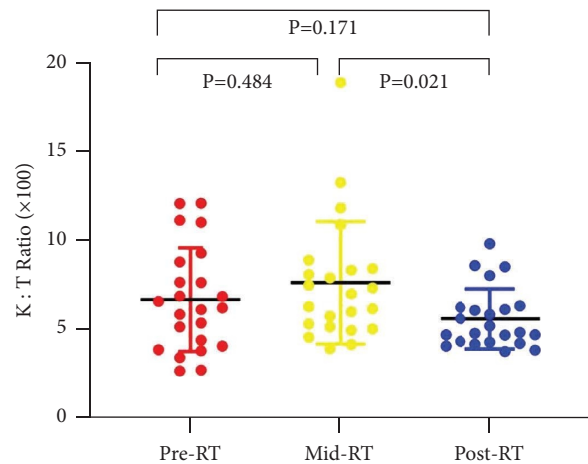


FIGURE 3: The levels of IDO activity at three time points during radiotherapy (before the initiation of RT, two weeks after the initiation of RT, and within one week after RT).

heterogeneously under different RT schemes due to the extent of immune activation [28, 29]. A study reported that IDO1 blockage could overcome radiation-induced “Rebound Immune Suppression” in the tumor microenvironment and sensitized Lewis lung carcinoma (LLC) tumors to hypo-fractionated RT [30]. Another study using the LLC model also revealed that the combination of IDO inhibitor 1-methyltryptophan (1-MT) and 10 Gy RT therapy was more effective than either treatment alone [31]. Intriguingly, Chen et al. found out that IDO1 blockade could protect the normal small intestinal epithelium from radiation toxicity in pre-clinical models [17]. Even though the relevant mechanism was unclear, the study shed light on related explorations, and it is promising to develop a more extensive usage of IDO1 inhibitors to increase efficacy and simultaneously decrease radiation-related toxicity in the future.

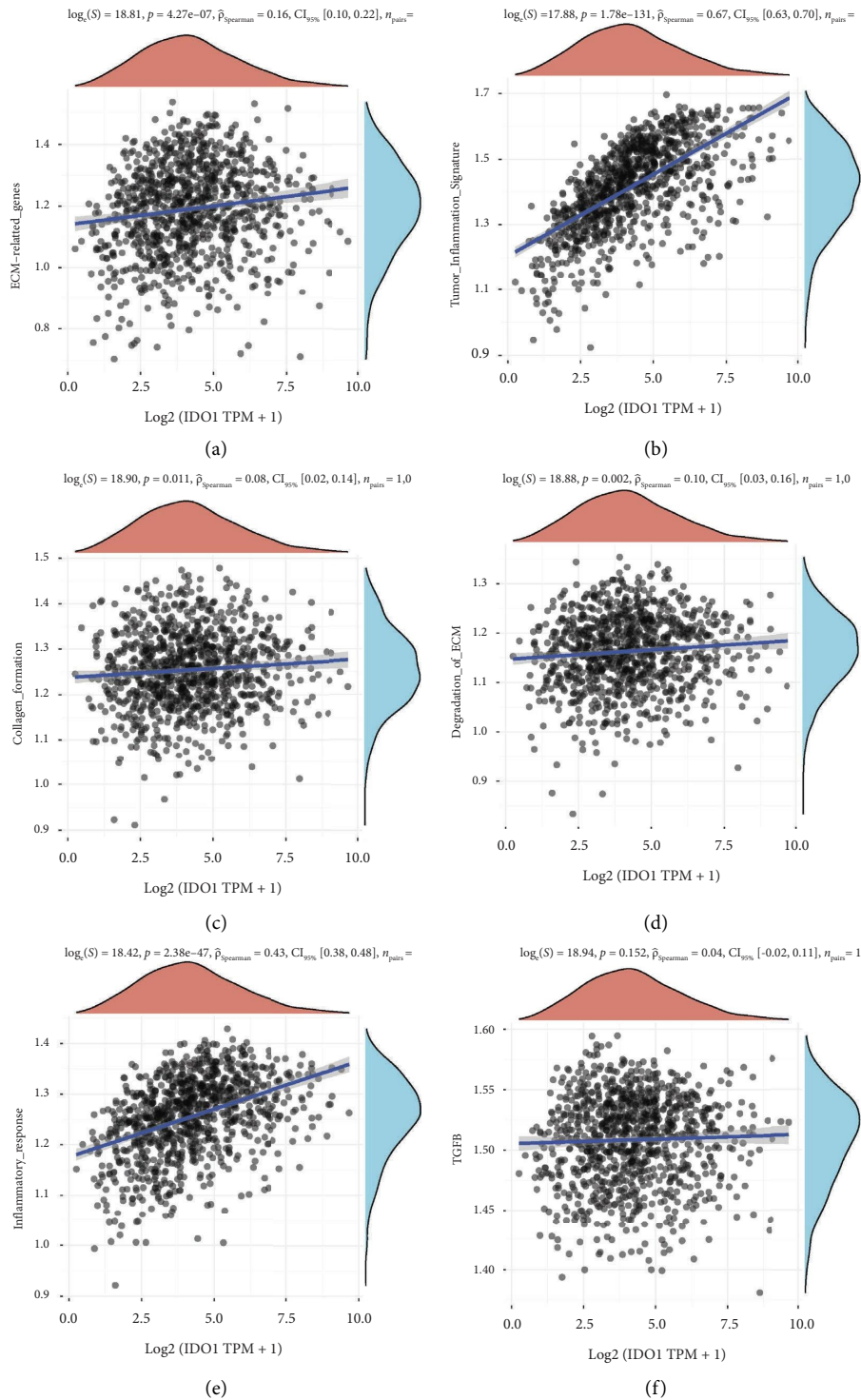


FIGURE 4: The correlation between IDO1 and pathway score was analyzed with Spearman. The abscissa represents the distribution of the gene expression, and the ordinate represents the distribution of the pathway score. The density curve on the right represents the trend in the distribution of pathway immune score, the upper density curve represents the trend in the distribution of the gene expression. The value on the top represents the correlation P value, correlation coefficient, and correlation calculation method. Six pathways are included: (a) ECM-related genes; (b) tumor inflammation signature; (c) collagen formation; (d) degradation of ECM; (e) inflammatory response; (f) TGFB.

The consensus on whether PETs parameters were predictive of RILT has not been reached yet. Wang et al. [11] reported poor baseline pulmonary function did not increase

the risk of symptomatic RILT in 260 NSCLC patients treated with CRT. On the contrary, Zhou et al. [32] concluded that a combination of DLCO% and MLD could predict the risk

for severe RP among patients with pretreatment moderate pulmonary dysfunction. A multicenter study demonstrated that FEV1, DLCO, and FeNO before CRT predict the development of G2 + RP [33]. Our study also showed that the addition of FEV1 could significantly increase the model's predictive ability for G3 + RILT. Besides, PETs are widely used in clinical practice with easily accessible data, so it is convenient to include PETs parameters in predictive models.

Our study has several limitations. Firstly, this study was performed in a single center, and only a small proportion of the participants' plasma was longitudinally followed. These results require further validation in a larger population among multiple centers. Secondly, this study only analyzed clinical characteristics, dosimetric factors, pulmonary function parameters, and metabolic data. A more comprehensive model of RILT incorporating genetic profiles and radiomics features warrants to be developed. Finally, since no patients in our cohort ever received immunotherapy, whether IDO1 activity could display similar predictive ability after consolidated immunotherapy is still unknown.

In conclusion, this study demonstrated that high baseline IDO1 activity combined with unfavorable baseline PETs was predictive of severe RILT in unresectable stage III NSCLC patients. IDO might mainly function in the early inflammatory phase of RILT development instead of the late fibrosis process. Finding effective interventions to alleviate RILT using IDO inhibitors is warranted in the future.

Data Availability

The data presented in this study are openly available at <https://www.ebi.ac.uk/metabolights/MTBLS5267>, with the accession number MTBLS5267.

Disclosure

Linfang Wu and Yibo Gao contributed equally as the first author.

Conflicts of Interest

The authors declare that they have no conflicts of interest.

Acknowledgments

This work was supported by the National Key R & D Program of China (grant nos. 2020AAA0109500 and 2021YFC2501900); National Natural Sciences Foundation of China (grant nos. 81872474, 82122053, and 81972316); Sanming Project of Medicine in Shenzhen (grant no. SZSM201612063); the Beijing Municipal Science and Technology Commission (grant no. Z191100006619118); CAMS Innovation Fund for Medical Sciences (CIFMS) (grant nos. 2021-I2M-1-067 and 2021-I2M-1-012); Non-profit Central Research Institute Fund of the Chinese Academy of Medical Sciences (grant nos. 2021-PT310-001 and 2021-RC310-020); the Key-Area Research and Development Program of Guangdong Province (grant no. 2021B0101420005).

References

- [1] R. Rosell and N. Karachaliou, "Large-scale screening for somatic mutations in lung cancer," *The Lancet*, vol. 387, no. 10026, pp. 1354–1356, 2016.
- [2] W. Chen, R. Zheng, P. D. Baade et al., "Cancer statistics in China, 2015," *CA: A Cancer Journal for Clinicians*, vol. 66, no. 2, pp. 115–132, 2016.
- [3] S. J. Antonia, A. Villegas, D. Daniel et al., "Durvalumab after chemoradiotherapy in stage III non-small-cell lung cancer," *New England Journal of Medicine*, vol. 377, no. 20, pp. 1919–1929, 2017.
- [4] L. Wu, S. Zhao, H. Huang, W. Wang, T. Zhang, Z. Zhou et al., "Treatment outcomes of patients with stage III non-small cell lung cancer and interstitial lung diseases receiving intensity-modulated radiation therapy: a single-center experience of 85 cases," *Thorac Cancer*, vol. 13, 2022.
- [5] A. Inoue, H. Kunitoh, I. Sekine, M. Sumi, K. Tokuyue, and N. Saijo, "Radiation pneumonitis in lung cancer patients: a retrospective study of risk factors and the long-term prognosis," *International Journal of Radiation Oncology, Biology, Physics*, vol. 49, no. 3, pp. 649–655, 2001.
- [6] J. H. Yu, Q. Y. Zhao, Y. Liu et al., "The plasma levels and polymorphisms of vitronectin predict radiation pneumonitis in patients with lung cancer receiving thoracic radiation therapy," *International Journal of Radiation Oncology, Biology, Physics*, vol. 110, no. 3, pp. 757–765, 2021.
- [7] G. Saito, Y. Oya, Y. Taniguchi et al., "Real-world survey of pneumonitis and its impact on durvalumab consolidation therapy in patients with non-small cell lung cancer who received chemoradiotherapy after durvalumab approval (HOPE-005/CRIMSON)," *Lung Cancer*, vol. 161, pp. 86–93, 2021.
- [8] X. Liu, C. Shao, and J. Fu, "Promising biomarkers of radiation-induced lung injury: a review," *Biomedicine*, vol. 9, no. 9, p. 1181, 2021.
- [9] M. Śliwińska-Mossoń, K. Wadowska, Ł. Trembecki, and I. Bil-Lula, "Markers useful in monitoring radiation-induced lung injury in lung cancer patients: a review," *Journal of Personalized Medicine*, vol. 10, no. 3, p. 72, 2020.
- [10] P. G. Hawkins, P. S. Boonstra, S. T. Hobson et al., "Radiation-induced lung toxicity in non-small-cell lung cancer: understanding the interactions of clinical factors and cytokines with the dose-toxicity relationship," *Radiotherapy and Oncology*, vol. 125, no. 1, pp. 66–72, 2017.
- [11] J. Wang, J. Cao, S. Yuan et al., "Poor baseline pulmonary function may not increase the risk of radiation-induced lung toxicity," *International Journal of Radiation Oncology, Biology, Physics*, vol. 85, no. 3, pp. 798–804, 2013.
- [12] L. Zhai, E. Ladomersky, A. Lenzen et al., "Ido1 in cancer: a Gemini of immune checkpoints," *Cellular and Molecular Immunology*, vol. 15, no. 5, pp. 447–457, 2018.
- [13] Y. C. Chen, X. L. He, L. Qi et al., "Myricetin inhibits interferon- γ -induced PD-L1 and Ido1 expression in lung cancer cells," *Biochemical Pharmacology*, vol. 197, Article ID 114940, 2022.
- [14] M. Mandarano, E. Orecchini, G. Bellezza et al., "Kynurenine/tryptophan ratio as a potential blood-based biomarker in non-small cell lung cancer," *International Journal of Molecular Sciences*, vol. 22, no. 9, p. 4403, 2021.
- [15] L. Loubaki, D. Chabot, and R. Bazin, "Involvement of the TNF- α /TGF- β /Ido axis in IVIg-induced immune tolerance," *Cytokine*, vol. 71, no. 2, pp. 181–187, 2015.

- [16] L. Wu, D. Wang, Y. Chen et al., “Dynamic Change of Ido1 Activity Predicts Survival in Patients with Unresectable Stage III NSCLC and Chemoradiotherapy,” *Frontiers in Immunology*, vol. 13, 2022.
- [17] B. Chen, D. M. Alvarado, M. Iticovici et al., “Interferon-induced Ido1 mediates radiation resistance and is a therapeutic target in colorectal cancer,” *Cancer immunology research*, vol. 8, no. 4, pp. 451–464, 2020.
- [18] Z. Zhang, J. Zhou, V. Verma et al., “Crossed pathways for radiation-induced and immunotherapy-related lung injury,” *Frontiers in Immunology*, vol. 12, Article ID 774807, 2021.
- [19] S. Aso, A. Navarro-Martin, R. Castillo et al., “Severity of radiation pneumonitis, from clinical, dosimetric and biological features: a pilot study,” *Radiation Oncology*, vol. 15, no. 1, p. 246, 2020.
- [20] B. K. Jeong, J. H. Kim, M. H. Jung, K. M. Kang, and Y. H. Lee, “Cytokine profiles of non-small cell lung cancer patients treated with concurrent chemoradiotherapy with regards to radiation pneumonitis severity,” *Journal of Clinical Medicine*, vol. 10, no. 4, p. 699, 2021.
- [21] X. Hu and L. B. Ivashkiv, “Cross-regulation of signaling pathways by interferon- γ : implications for immune responses and autoimmune diseases,” *Immunity*, vol. 31, no. 4, pp. 539–550, 2009.
- [22] E. S. Evans, Z. Kocak, S. M. Zhou et al., “Does transforming growth factor-beta1 predict for radiation-induced pneumonitis in patients treated for lung cancer?” *Cytokine*, vol. 35, no. 3-4, pp. 186–192, 2006.
- [23] J. P. Hart, G. Broadwater, Z. Rabbani et al., “Cytokine profiling for prediction of symptomatic radiation-induced lung injury,” *International Journal of Radiation Oncology, Biology, Physics*, vol. 63, no. 5, pp. 1448–1454, 2005.
- [24] F. Fallarino, U. Grohmann, and P. Puccetti, “Indoleamine 2,3-dioxygenase: from catalyst to signaling function,” *European Journal of Immunology*, vol. 42, no. 8, pp. 1932–1937, 2012.
- [25] M. T. Pallotta, C. Orabona, C. Volpi et al., “Indoleamine 2,3-dioxygenase is a signaling protein in long-term tolerance by dendritic cells,” *Nature Immunology*, vol. 12, no. 9, pp. 870–878, 2011.
- [26] S. Hänzelmann, R. Castelo, and J. Guinney, “GSVA: gene set variation analysis for microarray and RNA-seq data,” *BMC Bioinformatics*, vol. 14, no. 1, p. 7, 2013.
- [27] H. E. Barker, J. T. E. Paget, A. A. Khan, and K. J. Harrington, “The tumour microenvironment after radiotherapy: mechanisms of resistance and recurrence,” *Nature Reviews Cancer*, vol. 15, no. 7, pp. 409–425, 2015.
- [28] W. Wang, L. Huang, J. Y. Jin et al., “A validation study on Ido immune biomarkers for survival prediction in non-small cell lung cancer: radiation dose fractionation effect in early-stage disease,” *Clinical Cancer Research*, vol. 26, no. 1, pp. 282–289, 2020.
- [29] W. Wang, L. Huang, J. Y. Jin et al., “Ido immune status after chemoradiation may predict survival in lung cancer patients,” *Cancer Research*, vol. 78, no. 3, pp. 809–816, 2018.
- [30] A. Li, H. B. Barsoumian, J. E. Schoenhals et al., “Ido1 inhibition overcomes radiation-induced “rebound immune suppression” by reducing numbers of Ido1-expressing myeloid-derived suppressor cells in the tumor microenvironment,” *International Journal of Radiation Oncology, Biology, Physics*, vol. 104, no. 4, pp. 903–912, 2019.
- [31] M. Liu, Z. Li, W. Yao et al., “Ido inhibitor synergized with radiotherapy to delay tumor growth by reversing T cell exhaustion,” *Molecular Medicine Reports*, vol. 21, no. 1, pp. 445–453, 2020.
- [32] Y. Zhou, T. Yan, X. Zhou et al., “Acute severe radiation pneumonitis among non-small cell lung cancer (NSCLC) patients with moderate pulmonary dysfunction receiving definitive concurrent chemoradiotherapy: impact of pre-treatment pulmonary function parameters,” *Strahlentherapie und Onkologie*, vol. 196, no. 6, pp. 505–514, 2020.
- [33] L. Torre-Bouscoulet, W. R. Muñoz-Montaño, D. Martínez-Briseño et al., “Abnormal pulmonary function tests predict the development of radiation-induced pneumonitis in advanced non-small cell lung Cancer,” *Respiratory Research*, vol. 19, no. 1, p. 72, 2018.

Research Article

Long-Term Follow-Up Results of Adjuvant Intensity-Modulated Radiotherapy with Concurrent Paclitaxel and Cisplatin in High-Risk Endometrial Cancer Patients

Pei Shu , Xin Wang , Ganlu Ouyang , Jitao Zhou , Yaqin Zhao , Fang Wang ,
Zhiping Li , and Yali Shen 

Department of Abdominal Oncology, Cancer Center, West China Hospital, Sichuan University, No. 37 of Wainan Guoxue Lane, Chengdu, Sichuan Province, China 610041

Correspondence should be addressed to Yali Shen; sylprecious123@163.com

Received 30 July 2022; Revised 7 September 2022; Accepted 20 September 2022; Published 11 October 2022

Academic Editor: Ya Ju Hsieh

Copyright © 2022 Pei Shu et al. This is an open access article distributed under the Creative Commons Attribution License, which permits unrestricted use, distribution, and reproduction in any medium, provided the original work is properly cited.

Purpose. The purpose of this study was to retrospectively review the outcomes of patients with high-risk endometrial cancer treated with adjuvant radiotherapy with concurrent paclitaxel and cisplatin (TP). **Methods.** Patients with endometrial cancer who underwent radical surgery were screened between Jan 2005 and Dec 2018. Patients with high-risk factors who received adjuvant chemoradiotherapy were included in the study. High risks included stage I, endometrioid-type grade 3 with deep myometrial invasion or lymphovascular space invasion (or both), endometrioid-type stage II to IVa, or stage I to III with serous or clear cell histology. The adjuvant treatment regimen included one cycle of TP chemotherapy, followed by pelvic intensity-modulated radiotherapy (IMRT) with concurrent TP, followed by an additional one cycle of TP. Failure free survival (FFS) and overall survival (OS) were estimated. Patterns of recurrence and occurrence of adverse events were described. **Results.** A total of 450 patients with high-risk endometrial cancer were screened, 231 of whom were included in this study. After a median follow-up of 70 months, the 5-year OS was 94.7%, and the 6-year OS was 91.8%. The 5-y and 6-y FFS were 90.8% and 87.9%, respectively, which were related to stage ($P < 0.05$). A total of 14 patients experienced tumor recurrence, including 7 pelvic recurrence and 7 distant metastases. Seven patients died, all due to tumor progression. A total of 164 patients (71%) completed the prescribed course of treatment. A total of 205 patients had adverse events, 46 patients (20%) had grade 1, 92 patients (40%) had grade 2, 49 patients (21%) had grade 3, and 18 patients (8%) had grade 4. There were 83 nonhematologic and 122 hematologic toxicities (26 grade 3 and 18 grade 4). **Conclusion.** Adjuvant pelvic radiotherapy combined with synchronous TP chemotherapy can achieve excellent long-term survival for high-risk endometrial cancer patients. Moreover, this combination therapy has good safety and feasibility, which is worthy of further study and verification.

1. Introduction

Endometrial carcinoma is the sixth most common cancer in women, with 417,000 new cases and 97,000 deaths in 2020 worldwide [1]. Approximately 15% of patients with endometrial cancer have high-risk features, and most have poor outcomes [2, 3]. The risk of disease progression was significantly higher in high-risk patients than in non-high-risk patients who also received surgical treatment (local recurrence (13% vs. 5%) and distant recurrence (19% vs. 3%)) [4]. Therefore, adjuvant therapy was considered.

The PORTEC-1 and GOG 99 trials showed that adjuvant EBRT significantly reduced the risk of vaginal and pelvic relapse compared with observation (14% vs. 4% in PORTEC1, $P < 0.01$; 13% vs. 5% in GOG99, $P < 0.01$) [4, 5]. Based on these trials, radiation therapy was recommended to patients with high-risk features. However, adjuvant radiotherapy fails to improve the overall survival. Approximately 20% to 30% distant failure rates for high-risk patients with observation were reported in the PORTEC-1 and GOG 99 trials [4, 5]. Adjuvant chemotherapy was considered appropriate to investigate. The comparison of adjuvant

chemotherapy and pelvic EBRT was conducted in three randomized trials. The results showed that adjuvant chemotherapy reduced distant recurrence (16%-32% in chemotherapy versus 21%-38% in radiotherapy). The pelvic recurrence rate was lower in the radiotherapy group (18%-19% in the chemotherapy group versus 11%-13% in the radiotherapy group). Overall survival and relapse-free survival were similar between the two groups [6–8]. The complementarity of radiotherapy and chemotherapy is the basis for subsequent trials that focused on a combination of both in high-risk disease.

Five randomized clinical studies (Table 1) explored whether combination therapy could improve outcomes in high-risk endometrial cancer patients. In the pooled analysis of the NSGO 9501/EORTC 55991 trial and MaNGO ILLIAD-III trial, progression-free survival was 7% higher in the chemoradiotherapy group than in the radiotherapy group ($P = 0.009$), but no significant difference was noted in overall survival [9]. In the PORTEC-3 trial, survival benefit of 5% overall survival and 7% relapse-free survival was shown in the chemoradiotherapy group compared with the radiotherapy group [10]. However, GOG-249 and GOG-258 trials did not show improved relapse-free survival or overall survival in the chemoradiotherapy group compared to chemotherapy alone [11, 12]. The inconsistencies in the results highlight the importance of identifying the optimal adjuvant treatment for high-risk endometrial cancer.

The purpose of this study was to provide an optional treatment method for high-risk endometrial cancer patients. A single institutions' experience using postoperative pelvic intensity-modulated radiotherapy (IMRT) with paclitaxel and cisplatin (TP) concurrent chemotherapy was reported in this study.

2. Methods

2.1. Ethical Considerations. The study was approved by the Ethics Committee of West China Hospital, Sichuan University, China (No. 2020-748).

2.2. Patient Selection and Eligibility Criteria. A retrospective review was conducted for women with high-risk endometrial cancer from 2005 to 2018 in West China Hospital, Sichuan University. The review was performed to identify all patients with high-risk endometrial cancer treated with radical surgery. The high-risk endometrial cancer was considered as International Federation of Obstetrics and Gynecology (FIGO) 2009 stage I, endometrioid-type grade 3 with deep myometrial invasion or lymphovascular space invasion (or both), endometrioid-type stage II to IVa, or stage I to III with serous or clear cell histology.

Patients with high-risk endometrial cancer who had received adjuvant chemoradiotherapy (radiotherapy with concurrent paclitaxel and cisplatin chemotherapy) were included. Patients were excluded if they received single-modality adjuvant therapy such as chemotherapy or radiation therapy only or neither.

2.3. Treatment

2.3.1. Surgery. All patients had undergone total abdominal or laparoscopic hysterectomy with bilateral salpingo-oophorectomy and lymphadenectomy.

2.3.2. Chemotherapy. Patients received one cycle of the TP regimen (paclitaxel 175 mg/m², d1 and cisplatin 75 mg/m², d1), followed by two cycles of the TP regimen with a decreased dose (paclitaxel 90 mg/m², d1 and cisplatin 50 mg/m², d1, q3w) during radiotherapy. After completion of chemoradiotherapy (CRT), patients received one additional cycle of chemotherapy with a standard TP regimen.

2.3.3. Radiotherapy. Pelvic external-beam radiotherapy (EBRT) was given to patients after surgery. All patients were immobilized with abdominal body thermoplastic masks and treated in the supine position. Helical computed tomography at 3 mm slice thickness with intravenous contrast was performed for every patient. The clinical target volume (CTV) for radiotherapy was delineated according to the consensus guidelines for CTV delineation in postoperative pelvic radiation of endometrial and cervical cancer [13]. The clinical target volume included the upper 3 cm of the vagina, parametrial soft tissue, and pelvic regional lymph nodes (internal, external, and common iliac lymph nodes) up to the L5-S1 level. The clinical target volume was extended for lymph node involvement. A 0.6-0.8 cm uniform CTV expansion was applied to create the planning target volume (PTV).

A total dose of 50-50.4 Gy in 25-28 fractions was delivered. In patients with endometrioid-type grade 3 with both deep myometrial invasion and lymphovascular space invasion, an EBRT boost was given. A boost of 9 Gy/3 fractions was delivered to the upper two-thirds of the vagina, including the vaginal vault.

Plans were acceptable if the prescribed dose covered >95% of the PTV and no more than 1 cc received >107% of the prescribed dose. According to the Pelvic Normal Tissue Contouring Guidelines [14, 15], normal tissue constraints were as follows: less than 35% of the bladder to receive 50 Gy, less than 35% of the rectum to receive 50 Gy, less than 40% of the small bowel to receive 30 Gy, and less than 5% of the femoral heads to receive 50 Gy.

2.4. Follow-Up. Patients were followed up as scheduled: every 3 months for the first 2 years and every 6 months up to 5 years. Long-term outcome evaluation was obtained by follow-up visit. At each follow-up, a patient history, physical examination, and CA125 were performed. Radiologic assessments of chest and abdominal-pelvic were to be obtained every 6 months for the first 3 years and then annually for the next 2 years.

2.5. Outcomes. Analysis was performed to evaluate the effect of concurrent chemoradiotherapy. Overall survival (OS) was defined as the time from the date of surgery to the date of death from any cause. Failure-free survival (FFS) was defined as the interval between the date of surgery and the date of the first documentation of disease recurrence. Recurrences were analyzed according to the first site of recurrence.

Toxicity was assessed and graded with Common Terminology Criteria for Adverse Events (CTCAE) version 3.0.

2.6. Statistical Analysis. Descriptive statistics were used to quantify patient characteristics and toxicities. The Kaplan-Meier method was used to estimate overall and failure-free

TABLE 1: Summary of the main randomized controlled trials on adjuvant chemoradiotherapy for high-risk endometrial cancer.

Clinical trial	Number of patients	Treatment methods	Completion rate	LR	DM	5-year OS/DFS
PORTEC 3 ¹⁰	330	EBRT+ chemotherapy (consisting of two cycles of cisplatin 50 mg/m ² given during radiotherapy, followed by four cycles of carboplatin AUC 5 and paclitaxel 175 mg/m ²)	71%	1.3%	22.4%	81.8%/75.5%
GOG 258 ¹¹	346	EBRT + chemotherapy (consisting of two cycles of cisplatin 50 mg/m ² given during radiotherapy, followed by four cycles of carboplatin AUC 5 and paclitaxel 175 mg/m ²)	75%	13%	27%	76.8%/59%
NSGO/EORTC pooled with Iliade-III ⁹	267	EBRT+ chemotherapy (consisting of four cycles of AP or EP or TAC or TEC or TC)	72%	1%	6.6%	82%/78%
GOG 249 ¹²	300	VBT +chemotherapy (consisting of three cycles of carboplatin AUC 6 and paclitaxel 175 mg/m ²)	87%	9%	18%	85%/76%

LR: local recurrence; DM: distant metastasis; OS: overall survival; DFS: disease-free survival; EBRT: external-beam radiotherapy; AP: doxorubicin 50 mg/m² and cisplatin 50 mg/m²; EP: epirubicin 50 mg/m² and cisplatin 50 mg/m²; TAC: paclitaxel 175 mg/m² and doxorubicin 40 mg/m² plus carboplatin AUC 5; TEC: paclitaxel 175 mg/m² and epirubicin 50 mg/m² and carboplatin AUC 5; TC: paclitaxel 175 mg/m² and carboplatin AUC 5-6; VBT: vaginal brachytherapy.

survival. Univariate and multivariate Cox regression analyses were performed to determine the influence of covariates on survival. Statistical significance was defined as $P < 0.05$. All statistical analyses were performed using SPSS version 22.0 (IBM Corp., Armonk, NY, USA).

3. Results

From January 2005 to December 2018, 450 patients with high-risk endometrial cancer were reviewed. Patients were excluded if they received single-modality adjuvant therapy such as chemotherapy or radiation therapy only or neither, or they did not receive postoperative radiotherapy with concurrent chemotherapy with paclitaxel and cisplatin (TP) ($n = 219$). A total of 231 patients were enrolled and analyzed in this study. The median follow-up time for patients was 70 months (IQR 48.1-90.3 months), and 144 patients (62.3%) had reached at least 5 years of follow-up. The median age was 55 years (range 27-81 years). All patients had >1 of the high-risk factors, and 80% of them had FIGO 2009 stage II-III disease.

All patients underwent hysterectomy and lymph node removal. The median number of pelvic lymph node (LN) dissections was 22 (3-45). Pelvic nodal and para-aortic nodal involvement were detected in 39 patients (16.6%) and 5 patients (2.1%), respectively. The majority of histology was endometrioid (86.1%). Among them, grades 2 and 3 were present in 156 patients (67.5%). Other types of histology included adenosquamous carcinoma (10.8%) and serous histology (2.2%). On histologic examination, 77% of patients had lymphovascular space invasion, 35.5% of patients had deep myometrial invasion, and 15.6% of patients had both of them above. The baseline characteristics of the patients are given in Table 2.

All patients received pelvic IMRT. Five patients received extra para-aortic lymph node radiotherapy in addition to pelvic radiotherapy. Otherwise, a boost of 9 Gy/3 fractions was delivered to 21 patients. A total of 98.3% of patients (227/231) completed planned-dose radiotherapy. Only 4

patients received an external beam pelvic radiotherapy dose of 44-46 Gy due to toxicity.

One hundred sixty-four patients (71%) completed all cycles of chemotherapy. Due to hematologic toxicity, 44 (19%) and 18 (8%) patients required a dose reduction of cisplatin and paclitaxel, respectively. During radiotherapy, 11 (5%) patients did not receive concurrent chemotherapy for toxicity. Four cycles of chemotherapy were given to 164 patients, and 3 cycles of chemotherapy were delivered to 63 patients.

The median overall survival was still not reached, nor was the median failure-free survival. In total, 7 deaths occurred during the whole follow-up period. All deaths were related to the progression of endometrial cancer. The 3 y, 5 y, and 6 y OS rates were 96%, 94.7%, and 91.8%, respectively. The 3-y, 5-y, and 6-y FFS rates were 93.1%, 90.8%, and 87.9%, respectively. Figure 1 shows the OS and FFS curves.

Disease failure occurred in 14 (6%) patients. There were only 7 pelvic recurrences, which included 2 recurrences inside of the prior radiation field and 5 recurrences outside of the prior radiation field. The initial site of recurrence was extra-abdominal or hepatic in 6 patients. Only 1 patient had intrapelvic recurrence and synchronous distant metastasis together.

In univariate and multivariable analyses for OS and FFS, the following covariates were included: age, stage, histological type, grade, myometrial invasion, lymphovascular space invasion, and cervical junction involvement (Table 3). Univariate analysis showed that women with stage IIIC disease had much lower survival rates than those with stage I-IIIB disease. The five-year FFS and 5-year overall survival rates were 88.4% vs. 0% (HR 0.302, 95% CI 0.094-0.964; $P = 0.043$) and 97.4% versus 91.7% (HR 0.617, 95% CI 0.056-6.804; $P = 0.693$), respectively, for patients with different stages. In the multivariable analysis, none of the factors were significantly correlated with OS or FFS.

An overview of adverse events during and after treatment is provided in Table 4. Overall, adjuvant chemoradiotherapy was well tolerated. Most toxicities (60%) were grades

TABLE 2: Characteristics of patients ($n = 231$).

Variables	No. of patients (%)
Age (years), median (range)	55 (27-81)
FIGO 2009 stage	
Stage IA	9 (4)
Stage IB	33 (14.3)
Stage II	97 (42)
Stage IIIa	33 (14.3)
Stage IIIb	12 (5.2)
Stage IIIc	43 (18.6)
Stage IV	4 (1.7)
Histological grade and type	
EEC grade 1	43 (18.6)
EEC grade 2	73 (31.6)
EEC grade3	83 (35.9)
Serous	5 (2.2)
Adenosquamous cell carcinoma	25 (10.8)
Clear cell carcinoma	1 (0.4)
Neuroendocrine carcinoma	1 (0.4)
Myometrial invasion	
<50%	63 (27.3)
>50%	82 (35.5)
Missing	86 (37.2)
LVSI	
Yes	179 (77.5)
No	5 (2.2)
Unknown	47 (20.3)
Lymphode positive	39 (16.9)
Parametrium invasion	9 (3.9)

FIGO: International Federation of Obstetrics and Gynecology; EEC: endometrial endometrioid cancer; LVSI: lymph-vascular space invasion.

1-2. The rate of grade 3 or worse adverse events was reported to be 29%. During treatment, grade 3–4 acute adverse events were hematologic toxicities, which included grade 3-4 leukopenia or neutropenia in 35 patients and grade 3-4 anemia in 7 patients. Additionally, genitourinary (GU) or gastrointestinal (GI) adverse events were the second most common, occurring in 6 patients (2.6%) and 8 patients (3.5%), respectively. There was 1 patient with grade 3 liver damage recorded. There were no treatment-related deaths.

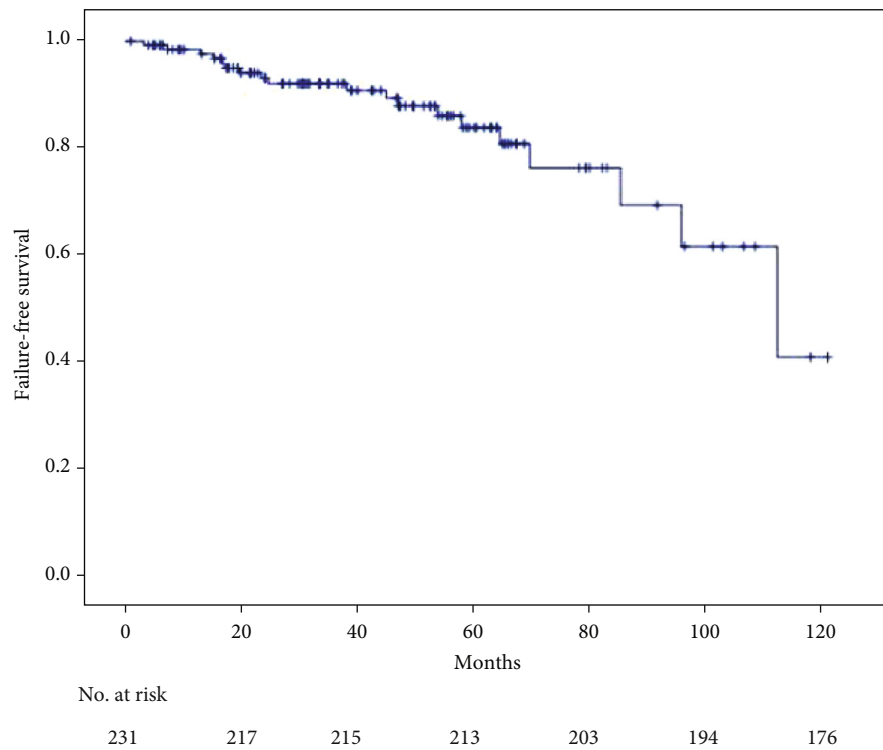
4. Discussion

To improve the prognosis of high-risk endometrial cancer (HREC), including local control and long-term survival, the role of adjuvant therapy needs to be further explored [16]. Phase III studies have shown that radiotherapy combined with chemotherapy can increase 5-y OS and FFS to 76.8%-85% and 59%-78% in high-risk endometrial cancer patients [11]. In this study, pelvic intensity-modulated radiotherapy (IMRT) combined with paclitaxel and cisplatin (TP) concurrent chemotherapy was applied, resulting in 5-y OS and FFS reaching 94.7% and 90.8%.

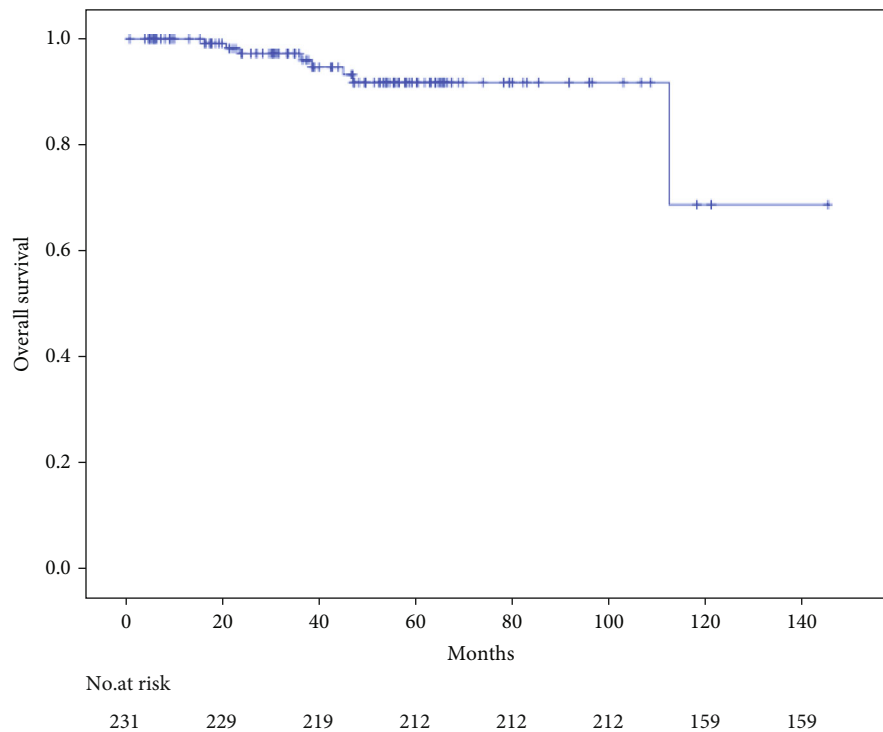
In different clinical trials, the specific implementation methods of radiotherapy and chemotherapy are different [9–12, 17, 18]. In the NSGO-EC-9501/EORTC-55991 trials, EBRT and four cycles of platinum-based chemotherapy given sequentially before or after EBRT were used [9]. In the clinical trial of PORTEC-3 and GOG 258, the treatment regimen was radiotherapy simultaneously with cisplatin, followed by paclitaxel and carboplatin for 4 cycles, which was the same as the RTOG-9708 trial [10, 11]. In the GOG 249 trial, vaginal brachytherapy followed by three cycles of carboplatin and paclitaxel was used [12]. In the RTOG 0921 trial, IMRT and concurrent cisplatin and bevacizumab followed by adjuvant carboplatin and paclitaxel for 4 cycles was used [17]. In this study, four cycles of TP chemotherapy were given, one cycle before radiotherapy, two cycles of TP chemotherapy simultaneously with pelvic IMRT, and one cycle of TP after radiotherapy. Different treatment regimens may bring differences in efficacy and side effects.

In the RTOG 0921 trial, adding bevacizumab to concurrent cisplatin-based chemoradiation increased the 2-year OS rate compared with previous study (97% vs. 90%) [17, 18]. Given this finding, it was postulated that the intensive concurrent treatment may further improve the outcome. Both cisplatin and paclitaxel were thought to have high activity in endometrial cancer and act as a radiation potentiator [19, 20]. The effects of adjuvant radiotherapy and concurrent cisplatin in high risk endometrial cancer have been revealed [11]. In addition, previous studies suggest that radiation with concurrent paclitaxel is well tolerated and effective for high-risk endometrial cancers [21, 22]. Paclitaxel plus platinum has been employed by Nomura et al. to evaluate the clinical benefit as postoperative adjuvant chemotherapy in endometrial cancer. The 5-year progression-free survival rate and 5-year overall survival rate were 73.9% and 86.1%, which were comparable with standard treatment [23]. Thus, the paclitaxel plus platinum regimen is an effective treatment for high-risk endometrial cancer. Given the impressive activity of paclitaxel and platinum in endometrial cancer and their radio-sensitizing properties, combination therapy of paclitaxel and cisplatin concurrent with radiotherapy is reasonable to explore [21, 24]. If TP regimen is given during radiotherapy, adverse events may increase with improved efficacy. Therefore, dose adjustment is the key when TP regimen is given simultaneously in radiotherapy. In this study, TP chemotherapy was given while in radiotherapy. The dose of the concurrent TP regimen was determined according to the tolerated dose obtained in the previous phase I study [25]. The tolerated dose of concurrent chemotherapy is paclitaxel 90 mg/m² and cisplatin 50 mg/m² [25].

As a precise irradiation technique, intensity-modulated radiotherapy (IMRT), compared with three-dimensional conformal radiotherapy (3D conformal radiotherapy), provide more accurate irradiation dose to the target region and better protection to adjacent normal organs. Reducing the irradiation range and dose to normal tissue can help reduce treatment-related toxicity [26, 27]. A study by Iğdem et al. showed a reduction in the volume of small bowel irradiated to more than 45 Gy with IMRT than with 4-field box radiation [28]. In the PORTEC-3 trial, which used 4-field



(a)



(b)

FIGURE 1: Kaplan-Meier survival curves for failure-free survival (a) and overall survival (b) in all patients.

conformal radiation, 14% of patients experienced grade 3 or 4 gastrointestinal toxicity [10]. In this study, the incidence of grade 3 and above gastrointestinal toxicity was 3.5% with IMRT.

Compared with other studies (listed in Table 1), the result of adverse events is acceptable in present study. In those phase III trials, the incidence of grade 3-4 toxicity was 51%-64.1%. In present study, the incidence of grade 3-

TABLE 3: Univariate prognostic factor analysis.

Factors	N	3 y-FFS (%)	P*	3 y-OS (%)	P*
Age (years)					
<60	156	90.5	0.726	95.1	0.812
60-69	58	96.4		95	
≥70	17	90.9		90	
T-category					
≤T2	149	92.3	0.05	100	0.497
>T3	82	64.3		80	
N-category					
N+	39	94.1	0.465	100	0.054
N-	192	75.9		89.1	
Stage					
I-IIIB	184	88.4	0.043	97.4	0.693
IIIC-IV	47	0		91.7	
Tumor grade					
G1-2	116	90	0.505	95.8	0.054
G3	115	90.6		100	
Myometrial invasion					
<50%	63	93.6	0.652	100	0.221
>50%	82	91.4		94.9	
Parametrium invasion					
Yes	9	87.4	0.947	96.2	0.532
No	107	100		100	
Cervical junction involvement					
Yes	96	92.2	0.384	98	0.055
No	39	85.2		88.2	

FFS: failure-free survival; OS: overall survival.

TABLE 4: Grade 3-4 acute toxicity.

AE	Grade 3 N (%)	Grade 4 N (%)
Gastrointestinal toxicity	8 (3.5%)	0
Hematologic toxicity		
Hemoglobin	3 (1%)	4 (2%)
Leukocyte	21 (9%)	14 (6%)
Platelet	2 (1%)	0
Diarrhea	3 (1%)	0
Fatigue	5 (2%)	0
Genitourinary	6 (2.6%)	0
Liver function	1 (1%)	0

AE: adverse event.

4 toxicity was much lower, 29.1%. The combined scheme is safe and feasible, making the treatment completion rate in this study reach 71%, which is similar to that of PORTEC-3 [10]. Therefore, lower toxicity and better completion rate are important guarantees for the good long-term prognosis of this study. In this study, the patterns of treatment failure include 7 cases of local recurrence and 7 cases of distant recurrence. A total of 7 cases died due to disease progression

during follow-up. In this study, the recurrence rate and mortality rate are low, indicating that the long-term treatment effect of high-risk endometrial patients is ideal. Given the small number of failure events, it is difficult to analyze the factors related to clinical outcome. Other studies have shown that staging is a prognostic factor for FFS, which is consistent with the conclusion of univariate analysis in this study [29].

Admittedly, this study has limitations. First, this is a retrospective study. Although more than 200 cases were included, there is still selection bias. In addition, this is a single-center study, and the treatment methods are relatively unified. It is impossible to compare the efficacy and safety with different radiotherapy and chemotherapy regimen. In the future, prospective clinical trials need to be carried out for research and verification. More trials should further address the use of concurrent treatment including chemotherapy or bevacizumab in patients with endometrial cancer.

5. Conclusions

This study showed that adjuvant pelvic radiotherapy combined with synchronous TP chemotherapy can achieve excellent long-term survival and good safety for high-risk endometrial cancer patients. It provides more clinical

evidence for recommending radiotherapy and chemotherapy as the standard adjuvant treatment for high-risk endometrial cancer.

Data Availability

The datasets analyzed during the current study can be obtained from the corresponding author on reasonable requirements.

Disclosure

Partial results of this study were presented as a conference abstract, which has been included in the “International Journal of Radiation Oncology Biology and Physics” (doi:10.1016/j.ijrobp.2019.06.1685).

Conflicts of Interest

The authors declare that they have no conflicts of interest.

Authors' Contributions

Yali Shen is responsible for the conception and design, collection and assembly of data, data analysis and interpretation, manuscript writing, and accountability for all aspects of the work; Pei Shu for the conception and design, provision of study material or patients, manuscript writing, and accountability for all aspects of the work; Xin Wang for the conception and design, provision of study material or patients, data analysis and interpretation, manuscript writing, and accountability for all aspects of the work; Ganlu Ouyang, Jitao Zhou, Yaqin Zhao, and Fang Wang for the provision of study material or patients, data analysis and interpretation, and accountability for all aspects of the work; and Zhiping Li for the provision of study material or patients and manuscript revision. All authors read and approved the final manuscript.

Acknowledgments

The authors would like to thank the ASTRO for the recognition of our research.

References

- [1] H. Sung, J. Ferlay, R. L. Siegel et al., “Global cancer statistics 2020: GLOBOCAN estimates of incidence and mortality worldwide for 36 cancers in 185 countries,” *CA: a Cancer Journal for Clinicians*, vol. 71, no. 3, pp. 209–249, 2021.
- [2] C. L. Creutzberg, W. van Putten, C. C. Wárlám-Rodenhuis et al., “Outcome of high-risk stage IC, grade 3, compared with stage I endometrial carcinoma patients: the postoperative radiation therapy in endometrial carcinoma trial,” *Journal of Clinical Oncology*, vol. 22, no. 7, pp. 1234–1241, 2004.
- [3] K. M. Greven, M. Randall, J. Fanning et al., “Patterns of failure in patients with stage I, grade 3 carcinoma of the endometrium,” *International Journal of Radiation Oncology • Biology • Physics*, vol. 19, no. 3, pp. 529–534, 1990.
- [4] H. M. Keys, J. A. Roberts, V. L. Brunetto et al., “A phase III trial of surgery with or without adjunctive external pelvic radiation therapy in intermediate risk endometrial adenocarcinoma: a gynecologic oncology group study,” *Gynecologic Oncology*, vol. 92, no. 3, pp. 744–751, 2004.
- [5] C. L. Creutzberg, W. L. J. van Putten, P. C. M. Koper et al., “Surgery and postoperative radiotherapy versus surgery alone for patients with stage-1 endometrial carcinoma: multicentre randomised trial,” *Lancet*, vol. 355, no. 9213, pp. 1404–1411, 2000.
- [6] R. Maggi, A. Lissoni, F. Spina et al., “Adjuvant chemotherapy vs_ radiotherapy in high-risk endometrial carcinoma: results of a randomised trial,” *British Journal of Cancer*, vol. 95, no. 3, pp. 266–271, 2006.
- [7] M. E. Randall, V. L. Filiaci, H. Muss et al., “Randomized phase III trial of whole-abdominal irradiation versus doxorubicin and cisplatin chemotherapy in advanced endometrial carcinoma: a gynecologic oncology group study,” *Journal of Clinical Oncology*, vol. 24, no. 1, pp. 36–44, 2006.
- [8] N. Susumu, S. Sagae, Y. Udagawa et al., “Randomized phase III trial of pelvic radiotherapy versus cisplatin-based combined chemotherapy in patients with intermediate- and high-risk endometrial cancer: a Japanese Gynecologic Oncology Group study,” *Gynecologic Oncology*, vol. 108, no. 1, pp. 226–233, 2008.
- [9] T. Hogberg, M. Signorelli, C. F. de Oliveira et al., “Sequential adjuvant chemotherapy and radiotherapy in endometrial cancer - results from two randomised studies,” *European Journal of Cancer*, vol. 46, no. 13, pp. 2422–2431, 2010.
- [10] S. M. de Boer, M. E. Powell, L. Mileschkin et al., “Adjuvant chemoradiotherapy versus radiotherapy alone for women with high-risk endometrial cancer (PORTEC-3): final results of an international, open-label, multicentre, randomised, phase 3 trial,” *The Lancet Oncology*, vol. 19, no. 3, pp. 295–309, 2018.
- [11] D. Matei, V. Filiaci, M. E. Randall et al., “Adjuvant chemotherapy plus radiation for locally advanced endometrial cancer,” *The New England Journal of Medicine*, vol. 380, no. 24, pp. 2317–2326, 2019.
- [12] M. E. Randall, V. Filiaci, D. S. McMeekin et al., “Phase III trial: adjuvant pelvic radiation therapy versus vaginal brachytherapy plus paclitaxel/carboplatin in high-intermediate and high-risk early stage endometrial cancer,” *Journal of Clinical Oncology*, vol. 37, no. 21, pp. 1810–1818, 2019.
- [13] W. Small, L. K. Mell, P. Anderson et al., “Consensus guidelines for delineation of clinical target volume for intensity-modulated pelvic radiotherapy in postoperative treatment of endometrial and cervical cancer,” *International Journal of Radiation Oncology • Biology • Physics*, vol. 71, no. 2, pp. 428–434, 2008.
- [14] H. A. Gay, H. J. Barthold, E. O'Meara et al., “Pelvic normal tissue contouring guidelines for radiation therapy: a radiation therapy oncology group consensus panel atlas,” *International Journal of Radiation Oncology • Biology • Physics*, vol. 83, no. 3, pp. e353–e362, 2012.
- [15] B. Emami, J. Lyman, A. Brown et al., “Tolerance of normal tissue to therapeutic irradiation,” *International Journal of Radiation Oncology • Biology • Physics*, vol. 21, no. 1, pp. 109–122, 1991.
- [16] K. Albuquerque, J. Chino, A. Klopp, M. Kamrava, and S. Beriwal, “Defining the place of adjuvant chemotherapy and radiation for high-risk endometrial cancer from recent randomized clinical trials: some answers, more questions,” *International Journal of Radiation Oncology • Biology • Physics*, vol. 102, no. 3, pp. 473–477, 2018.

- [17] A. N. Viswanathan, J. Moughan, B. E. Miller et al., “NRG oncology/RTOG 0921: a phase 2 study of postoperative intensity-modulated radiotherapy with concurrent cisplatin and bevacizumab followed by carboplatin and paclitaxel for patients with endometrial cancer,” *Cancer*, vol. 121, no. 13, pp. 2156–2163, 2015.
- [18] S. A. Milgrom, M. A. Kollmeier, N. R. Abu-Rustum et al., “Postoperative external beam radiation therapy and concurrent cisplatin followed by carboplatin/paclitaxel for stage III (FIGO 2009) endometrial cancer,” *Gynecologic Oncology*, vol. 130, no. 3, pp. 436–440, 2013.
- [19] H. G. Ball, J. A. Blessing, S. S. Lentz, and D. G. Mutch, “A phase II trial of paclitaxel in patients with advanced or recurrent adenocarcinoma of the endometrium: a gynecologic oncology group study,” *Gynecologic Oncology*, vol. 62, no. 2, pp. 278–281, 1996.
- [20] H. Choy, F. F. Rodriguez, S. Koester, S. Hilsenbeck, and D. D. von Hoff, “Investigation of taxol as a potential radiation sensitizer,” *Cancer*, vol. 71, no. 11, pp. 3774–3778, 1993.
- [21] H. Cho, B. H. Nam, S. M. Kim et al., “A phase 2 trial of radiation therapy with concurrent paclitaxel chemotherapy after surgery in patients with high-risk endometrial cancer: a Korean Gynecologic Oncologic Group study,” *International Journal of Radiation Oncology • Biology • Physics*, vol. 90, no. 1, pp. 140–146, 2014.
- [22] L. Frigerio, G. Mangili, G. Aletti et al., “Concomitant radiotherapy and paclitaxel for high-risk endometrial cancer: first feasibility study,” *Gynecologic Oncology*, vol. 81, no. 1, pp. 53–57, 2001.
- [23] H. Nomura, D. Aoki, H. Michimae et al., “Effect of taxane plus platinum regimens vs doxorubicin plus cisplatin as adjuvant chemotherapy for endometrial cancer at a high risk of progression: a randomized clinical trial,” *JAMA Oncology*, vol. 5, no. 6, pp. 833–840, 2019.
- [24] S. Lincoln, J. A. Blessing, R. B. Lee, and T. F. Rocereto, “Activity of paclitaxel as second-line chemotherapy in endometrial carcinoma: a gynecologic oncology group study,” *Gynecologic Oncology*, vol. 88, no. 3, pp. 277–281, 2003.
- [25] P. Shu, Y. Shen, Y. Zhao et al., “A phase I study of adjuvant intensity-modulated radiotherapy with concurrent paclitaxel and cisplatin for cervical cancer patients with high risk factors,” *Medical Oncology*, vol. 32, no. 11, p. 247, 2015.
- [26] J. C. Roeske, D. Bonta, L. K. Mell, A. E. Lujan, and A. J. Mundt, “A dosimetric analysis of acute gastrointestinal toxicity in women receiving intensity-modulated whole-pelvic radiation therapy,” *Radiotherapy and Oncology*, vol. 69, no. 2, pp. 201–207, 2003.
- [27] A. J. Mundt, L. K. Mell, and J. C. Roeske, “Preliminary analysis of chronic gastrointestinal toxicity in gynecology patients treated with intensity-modulated whole pelvic radiation therapy,” *International Journal of Radiation Oncology • Biology • Physics*, vol. 56, no. 5, pp. 1354–1360, 2003.
- [28] T. Ercan, G. Alço, F. Zengin et al., “Dosimetric comparison of intensity modulated pelvic radiotherapy with 3D conformal radiotherapy in patients with gynecologic malignancies,” *European Journal of Gynaecological Oncology*, vol. 30, no. 5, pp. 547–551, 2009.
- [29] H. D. Homesley, V. Filiaci, S. K. Gibbons et al., “A randomized phase III trial in advanced endometrial carcinoma of surgery and volume directed radiation followed by cisplatin and doxorubicin with or without paclitaxel: a gynecologic oncology group study,” *Gynecologic Oncology*, vol. 112, no. 3, pp. 543–552, 2009.

Research Article

miR-3059-3p Regulates Glioblastoma Multiforme Radiosensitivity Enhancement through the Homologous Recombination Pathway of DNA Repair

Yu-Wen Cheng,^{1,2} Chien-Ju Lin,³ Shih-Hsun Kuo,⁴ Ann-Shung Lieu,^{5,6} Chee-Yin Chai,^{2,7,8} Hung-Pei Tsai ⁵ and Aij-Lie Kwan ^{2,5,6,9}

¹Department of Neurosurgery, Kaohsiung Veterans General Hospital, Kaohsiung, Taiwan

²Graduate Institute of Medicine, College of Medicine, Kaohsiung Medical University, Kaohsiung, Taiwan

³School of Pharmacy, College of Pharmacy, Kaohsiung Medical University, Kaohsiung, Taiwan

⁴Department of Radiation Oncology, Kaohsiung Medical University Hospital, Kaohsiung, Taiwan

⁵Division of Neurosurgery, Department of Surgery, Kaohsiung Medical University Hospital, Kaohsiung, Taiwan

⁶Department of Surgery, School of Medicine, College of Medicine, Kaohsiung Medical University, Kaohsiung, Taiwan

⁷Department of Pathology, Kaohsiung Medical University Hospital, Kaohsiung, Taiwan

⁸Department of Pathology, School of Medicine, College of Medicine, Kaohsiung Medical University, Kaohsiung, Taiwan

⁹Department of Neurosurgery, University of Virginia, Charlottesville, VA, USA

Correspondence should be addressed to Hung-Pei Tsai; carbugino@gmail.com and Aij-Lie Kwan; aijliekwan@yahoo.com.tw

Received 24 June 2022; Accepted 7 September 2022; Published 21 September 2022

Academic Editor: Xiangya Ding

Copyright © 2022 Yu-Wen Cheng et al. This is an open access article distributed under the Creative Commons Attribution License, which permits unrestricted use, distribution, and reproduction in any medium, provided the original work is properly cited.

Background. Glioblastoma multiforme (GBM) is one of the most deadly and recalcitrant illnesses of the neurocentral nervous system in humans. MicroRNAs (miRNAs) are a class of noncoding RNAs that play important roles in the regulation of gene expression and biological processes, including radiosensitivity. In this study, we demonstrated the relationship between miR-3059-3p and radiation in GBM. **Materials and Methods.** Radioresistant (RR) cells were obtained by exposing GBM8401 cells to 80 Gy radiation in 20 weekly 4 Gy fractions. miR-3059-3p mRNA and DNA replication helicase/nuclease 2 (DNA2) protein expressions were detected using real-time polymerase chain reaction and immunoblotting. Using flow cytometry, colony formation and apoptosis were identified using miR-3059-3p mimic, miR-3059-3p inhibitor, DNA2 siRNA, and DNA2 plasmid. Immunoblotting was used to detect DNA repair proteins. **Results.** Low levels of miR-3059-3p and high levels of DNA2 were observed in RR cells. Colony formation and apoptosis assays revealed that miR-3059-3p targeted DNA2 to regulate radioresistance. Immunoblotting revealed that miR-3059-3p regulated the homologous recombination (HR) pathway (Rad51 and Rad52) but not the nonhomologous end joining pathway (ku70 and ku80). **Conclusion.** Downregulation of DNA2 via miR-3059-3p enhanced the radiosensitivity of GBM cells through the inhibition of the HR pathway.

1. Introduction

Glioblastoma multiforme (GBM) in humans is one of the most deadly and recalcitrant illnesses of the neurocentral nervous system. Approximately 12,120 patients in the United States alone were diagnosed with GBM in 2016 with a 5-year survival rate of 5%, and the peak age-adjusted inci-

dence of GBM is estimated to be 3.2 per 100,000 [1]. The exact etiology of the disease is currently unknown, and only limited well-established research has indicated radiation as the cause [2]. Clinical results of GBM may present some obvious symptoms, including persistent weakness, numbness, loss of vision, or changes in language based on the neurological function. As the tumor size increases, symptoms

such as headache, nausea, vomiting, and even loss of consciousness also appear. Magnetic resonance imaging is the standard radiographic imaging modality in the diagnosis and posttreatment management of patients with glioblastoma [3]. Current treatment approaches include surgical resection with radiotherapy (RT) as well as concomitant and maintenance chemotherapy, such as temozolomide [4]. The overall survival is still dismal, and the average survival time is <2 years [5, 6]. Despite advancements in neurosurgery and RT, the development of potent chemotherapeutic drugs, and comprehensive genomic profiling and molecular diagnostics over the last several decades, there has been little improvement in increasing the overall survival rate [7].

Radioresistance (RR) is responsible for the poor therapeutic effect of RT on GBM tumors. GBM cells exhibit increased proliferation and insufficient vascularization, which induces local hypoxia in tumor sites [8, 9]. Moreover, hypoxia is well known to play an important role in RR. Additionally, fractionated RT, epithelial–mesenchymal transition, and cancer stem cells can induce RR [10, 11]. Therefore, inhibiting RR can improve the therapeutic effect of RT on GBM tumors.

MicroRNAs (miRNAs) are noncoding RNAs that play an important role in regulating mRNA expressions. The average length of a miRNA molecule is 22 nucleotides. They are transcribed from DNA sequences into primary miRNAs (pri-miRNAs) and processed into precursor miRNAs (pre-miRNAs), which then mature into miRNAs. miRNAs have been shown to regulate gene expressions following binding to the 3'-untranslated region of target mRNAs to induce mRNA degradation or translational repression [12–14]. Recent studies have shown that miRNAs can regulate RR by targeting mRNAs to mediate many biological processes, including proliferation, cell cycle, aging, apoptosis, and DNA repair [15–19]. Several studies have shown that microRNAs can regulate the therapeutic effect of radiation. For example, miR-409-3p mediated radiosensitivity in non-small-cell lung cancer [20]. miR-31 induced RR by regulating reactive oxygen species in pancreatic ductal adenocarcinoma [21]. In addition, the tumor environment is associated with radioresistance. In colorectal cancer, exosomal miR-590-3p from cancer-associated fibroblasts regulated radioresistance [22]. At present, miR-3059-3p has been shown to regulate stress-induced depression and resilience [23]. However, there are no reports on the relationship between miR-3059-3p and radiation. This study is therefore aimed at investigating the relationship between miR-3059-3p and radiosensitivity and the underlying mechanisms.

2. Materials and Methods

2.1. Cell Culture. GBM8401 cells were obtained from the Bioresource Collection and Research Center and cultured in RPMI medium supplemented with 10% fetal bovine serum under 5% CO₂ atmosphere at 37°C. The cells were exposed to 80 Gy radiation in 20 weekly 4 Gy fractions to yield RR cells.

2.2. Colony Formation. GBM cells were seeded into 6-well plates at a density of 100, 200, 400, 1000, and 10,000 cells per well and exposed to radiation doses of 0, 1, 2, 4, and 8 Gy, respectively. A linear accelerator was used to irradiate cells, which was performed at room temperature. The cells were stained with 0.5% crystal violet after a 10-day incubation. The number of colonies formed was normalized to plating efficiency (PE) and represented as a surviving fraction (SF) relative to the control. The PE and SF were calculated as follows: PE = (number of colonies formed/number of inoculated cells) × 100%; SF = number of colonies formed/(number of seeded cells × [PE/100]).

2.3. Transfection. MicroRNA was transfected into GBM8401 cells using DharmaFECT transfection reagents (Dharmacon™, Lafayette, USA). Transfection was performed using 5 μM microRNA mimic/inhibitor or DNA replication helicase/nuclease 2 (DNA2) siRNA/plasmid for 2 days. The following microRNAs were used: miRNA mimic negative control sense UCACAACCUCCUGAAAGAGUAGA, miRNA mimic negative control antisense UCUACUCUUUCUAGGAGGUUGUGA, miRNA inhibitor negative control antisense UCUACUCUUUCUAGGAGGUUGUGA, miR-3059-3p mimic sense CCUCUAGGGAAGAGAA GGUUGG, miR-3059-3p mimic sense CCAACCUUCUC UUCCCUAGAGG, and miR-3059-3p inhibitor antisense CCAACCUUCUCUCCCUAGAGG.

2.4. MicroRNA Polymerase Chain Reaction (PCR). MicroRNAs were extracted and purified using the miRNeasy Mini kit (Qiagen, Hilden, Germany). miRNA expression levels were measured via quantitative reverse transcription-(qRT-) PCR using StepOne (Thermo, Waltham, USA). The cycling conditions were as follows: 95°C for 10 min, followed by 40 cycles of amplification at 95°C for 15 s, and 60°C for 60 s. The relative miR-3059-3p expression level was calculated using the 2^{-ΔΔCt} method. U6 was used as an internal control.

2.5. Immunoblotting. The cells were lysed with RIPA buffer, and 50 μg of protein per sample was loaded into the wells of a 10%–12% sodium dodecyl sulfate–polyacrylamide gel electrophoresis gel and electrophoresed at 70 and 110 V for 1 h each. The proteins were transferred to a polyvinylidene fluoride membrane following electrophoresing at 400 mA for 2 h. The membranes were blocked with blocking buffer for 1 h and incubated overnight with the respective primary antibody (β-actin (1:20,000; Sigma-Aldrich; A5411), Rad51 (1:1000; GeneTex; GTX70230), Rad52 (1:1000; SANTA CRUZ; sc-365341), Ku70 (1:1000; Arigo; ARG57851), Ku80 (1:1000; Arigo; ARG57867), and DNA2 (1:1000; Merck; HPA057526)) at 4°C, followed by incubation with the corresponding secondary antibody (goat anti-rabbit (1:5000; Millipore; AP132P) and goat anti-mouse (1:5000; Millipore; AP124P)) for 90 min. An enhanced chemiluminescence solution (Western Lightning; 205-14621) was used for detecting specific bands using the Mini Chemiluminescent Imaging and Analysis System (MINI-CHEMI; Beijing; China).

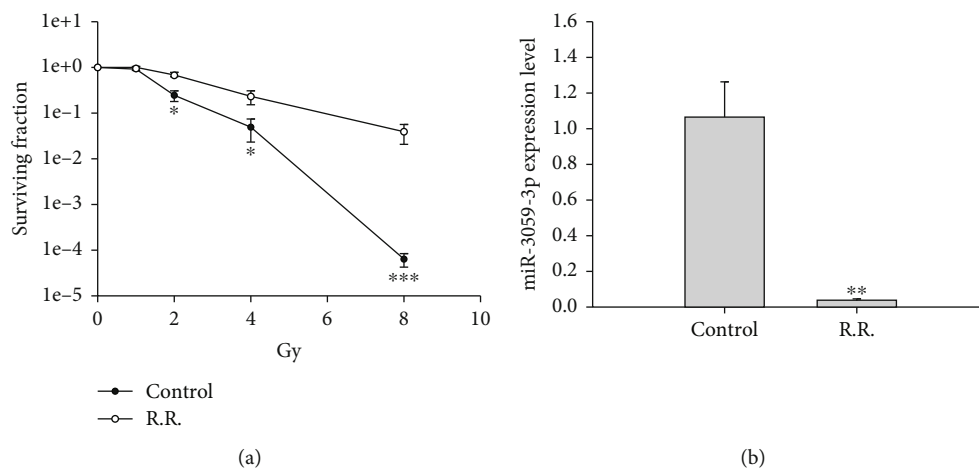


FIGURE 1: Colony formation and miR-3059-3p expression in RR cells. (a) Comparison of the surviving fraction between the RR and control groups receiving 0, 1, 2, 4, and 8 Gy radiation. (b) Real-time polymerase chain reaction was performed to analyze the expression level of miR-3059-3p, which was compared between the RR and control groups. * $P < 0.05$, ** $P < 0.01$, and *** $P < 0.001$ compared with controls. RR: radioresistant.

2.6. Flow Cytometry. A total of 1.5×10^5 GBM8401 cells were seeded into 6-well plates and incubated for 24 h followed by transfection with microRNA mimic, microRNA inhibitor, DNA2 siRNA, or DNA2 plasmid for 48 h and exposed to radiation. Both detached and attached cells were centrifuged at 1500 rpm for 5 min. Cells were washed once with phosphate-buffered saline and analyzed using the Muse® Annexin V and Dead Cell Assay Kit (Millipore, MCH100105, Burlington, USA).

2.7. Data Analysis. The SPSS 24.0 (IBM, NY, USA) software was used for statistical analysis. A one-way analysis of variance followed by Tukey's post hoc test was used to analyze the results of colony formation, apoptosis percentage, and western blot. For all analyses, a P value of < 0.05 was considered statistically significant.

3. Results

3.1. miR-3059-3p Expression in RR GBM Cells. To confirm the effect of miR-3059-3p on RR cells, we first evaluated SF under 0, 1, 2, 4, and 8 Gy radiation between the control and RR groups in GBM8401 cells. The results revealed that the RR group had a higher SF than the control group at 2 ($P < 0.05$), 4 ($P < 0.05$), and 8 ($P < 0.001$) Gy radiation (Figure 1(a)). miR-3059-3p expression was also detected in both groups, as revealed through qRT-PCR, where the RR group exhibited lower miR-3059-3p expression levels than the control group ($P < 0.01$) (Figure 1(b)). Therefore, miR-3059-3p may play an important role in radiosensitivity.

3.2. miR-3059-3p Enhanced Radiosensitivity in GBM8401 Cells after Radiation. The role of miR-3059-3p in radiosensitivity was further investigated. We evaluated the SF after radiation in miR-3059-3p mimic, miR-3059-3p inhibitor, miR mimic negative control, miR inhibitor negative control, and control groups in GBM8401 cells. The SF did not differ significantly between the control, miR mimic negative con-

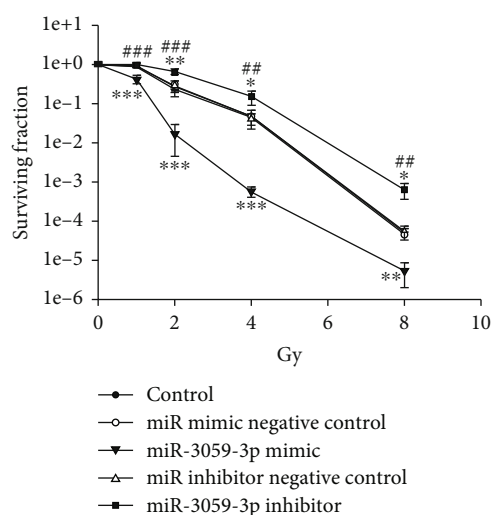


FIGURE 2: The surviving fraction of irradiated GBM cells with miR-3059-3p mimic or inhibitor. Comparison of the surviving fractions between the control, miR-3059-3p mimic, and miR-3059-3p inhibitor groups using colony formation assays in GBM8401 cells. ** $P < 0.01$ and *** $P < 0.001$ compared with the control group. ## $P < 0.01$ and ### $P < 0.001$ compared with the miR-3059-3p mimic group. GBM: glioblastoma multiforme.

trol, and miR inhibitor negative control groups. Compared with the other mimics, inhibitors, and controls, the miR-3059-3p inhibitor increased the number of colonies formed while miR-3059-3p mimic decreased it at 1 ($P < 0.001$), 2 ($P < 0.001$), 4 ($P < 0.001$), and 8 ($P < 0.001$) Gy radiation (Figure 2). These findings showed that miR-3059-3p regulated radiosensitivity in GBM cells. To confirm the therapeutic effect of radiation with miR-3059-3p, an apoptosis assay was performed in GBM8401 cells exposed to radiation using flow cytometry. The results indicated that the miR-3059-3p mimic group had a greater percentage of apoptotic cells than

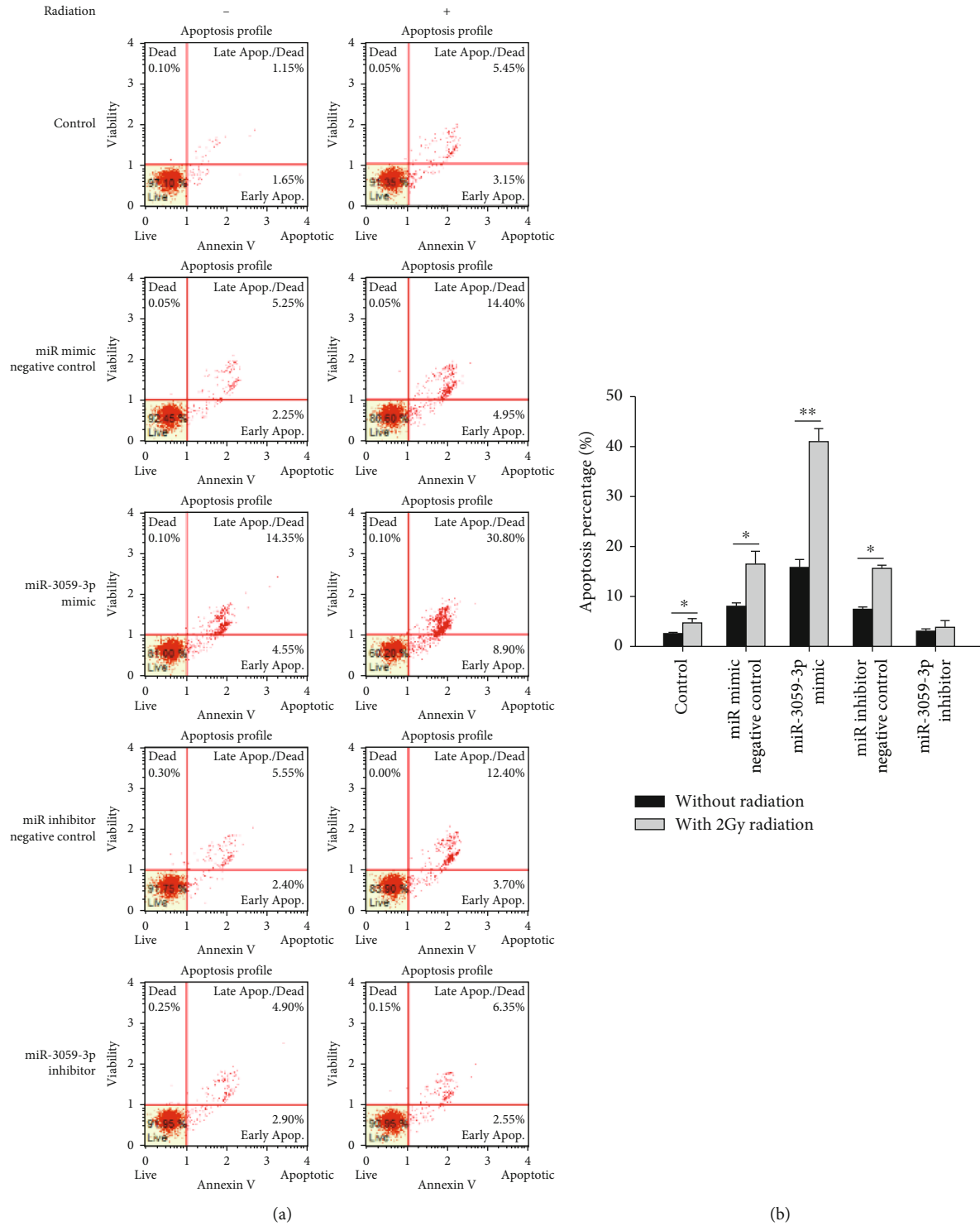


FIGURE 3: Apoptosis assay for miR-3059-3p with radiation. (a) Apoptosis of cells was determined via flow cytometry. (b) The percentage of apoptotic cells. * $P < 0.05$ and ** $P < 0.01$.

the control and miR-3059-3p mimic negative control groups after 2 Gy radiation (Figure 3(a)). The apoptosis percentages of the control, miR mimic negative control, miR-3059-3p mimic, miR inhibitor negative control, and miR-3059-3p inhibitor groups without radiation were $2.57\% \pm 0.21\%$, $7.9\% \pm 0.76\%$, $15.8\% \pm 1.59\%$, $7.3\% \pm 0.54\%$, and $3.0\% \pm 0.49$

$\%$, respectively. After 2 Gy radiation, these values were $4.6\% \pm 0.93\%$, $16.4\% \pm 2.64\%$, $40.9\% \pm 2.71\%$, $15.5\% \pm 0.74\%$, and $3.8 \pm 1.42\%$, respectively. Afterward, the miR-3059-3p mimic group showed significantly higher apoptosis than the other groups with 2 Gy radiation. In the control, miR mimic negative control, and miR inhibitor control groups,

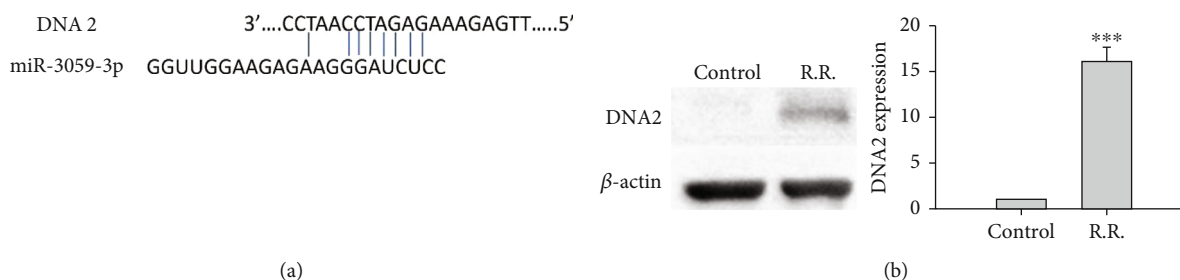


FIGURE 4: The target of miR-3059-3p. (a) The binding relation between miR-3059-3p and DNA2 was predicted using miRDB, an online database for miRNA target prediction and functional annotations. (b) In immunoblotting, the RR group showed higher DNA2 expression. *** $P < 0.001$ than the control group.

2 Gy radiation led to a twofold increase in the percentage of apoptosis cells. Transfection with miR-3059-3p mimic resulted in a 2.59-fold increase in apoptosis cells after 2 Gy radiation. However, transfection with miR-3059-3p inhibitor only showed a 1.25-fold increase (Figure 3(b)). These data suggest that miR-3059-3p can regulate radiation-induced apoptosis.

3.3. Mechanism of miR-3059-3p-Mediated Effects in RR GBM Cells. We further predicted the presence of a binding site between DNA2 and miR-3059-3p using miRDB [24], an online database for miRNA target prediction and functional annotations (Figure 4(a)), to clarify the role of DNA2 in RR *in vitro*. Moreover, DNA2 expression patterns in GBM8401 cells were detected using immunoblotting, and a higher DNA2 expression level was found in the RR group than in the control group ($P < 0.001$) (Figure 4(b)). To confirm the mechanism of miR-3059-3p in radiation, we transfected DNA2 siRNA or plasmid including miR-3059-3p mimic into GBM8401 cells and then evaluated the SF after radiation. miR-3059-3p mimic group showed a lower SF than the control group, as described above. The miR-3059-3p + DNA2 siRNA group exhibited the lowest SF, and the miR-3059-3p with DNA2 plasmid rescued the SF, with the level being nearly identical to that of the control group (Figure 5). We analyzed the apoptosis fraction among different combinations of miR-3059-3p and DNA2 after radiation exposure using flow cytometry. We found an increase in the percentage of apoptotic cells after radiation, which confirmed the effect of DNA2 downregulation (Figure 6(a)). The control group had $3.4\% \pm 0.56\%$ apoptotic cells. After 2 Gy radiation, the percentages of apoptosis cells in the control, miR-3059-3p mimic, miR-3059-3p mimic + DNA2 siRNA, miR-3059-3p + DNA2 plasmid, miR-3059-3p inhibitor + DNA2 plasmid, and miR-3059-3p inhibitor + DNA2 plasmid groups were $3.4\% \pm 0.57\%$, $8.6\% \pm 0.60\%$, $30.2\% \pm 1.43\%$, $44.2\% \pm 3.9\%$, $15.4\% \pm 1.42\%$, $16.5\% \pm 2.05\%$, and $4.4\% \pm 1.18\%$, respectively. The miR-3059-3p mimic + DNA2 siRNA group had the highest percentage of apoptotic GBM8401 cells (Figure 6(b)).

3.4. miR-3059-3p Attenuated the HR Pathway to Reduce DNA Repair via Targeting DNA2. Both HR and nonhomologous end-joining (NHEJ) are the main pathways in double-strand break (DSB) repair. RAD51 and RAD52 play key

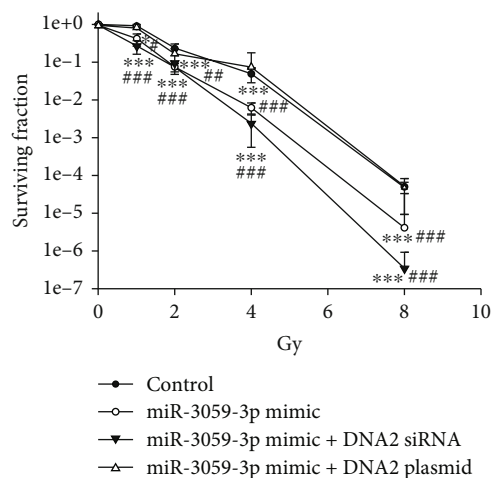


FIGURE 5: The miR-3059-3p mimic + DNA2 siRNA group showed a significantly low survival percentage. * $P < 0.05$ and *** $P < 0.001$ compared with the control group. ## $P < 0.01$ and ### $P < 0.001$ compared with the miR-3059-3p + DNA2 plasmid group.

roles in HR pathway-mediated DNA repair. RAD51 was mediated on ssDNA in a form that is active for homologous pairing and strand invasion in humans. RAD51 also regulates dsDNA and prevents dissociation from ssDNA. RAD52 plays another crucial role in the repair of DNA DSBs at the active transcription sites during the G0/G1 phase of the cell cycle. Repair of these DSBs appears to use an RNA template-based recombination mechanism dependent on RAD52. In the NHEJ pathway, the KU70/80 heterodimer plays a vital role as it binds to DNA termini with high affinity, thereby protecting DNA ends from degradation, and recruits other NHEJ factors required for repair [25]. We used immunoblotting to determine which DNA repair pathway DNA2 could take. The results revealed that the protein expressions of Ku80 and Ku70 were similar in each group, but in the miR-3059-3p mimic and miR-3059-3p mimic + DNA2 siRNA groups, the protein expressions of both RAD52 and RAD51 were low. miR-3059-3p mimic + DNA2 plasmid, miR-3059-3p inhibitor + DNA2 siRNA, and miR-3059-3p inhibitor + DNA2 plasmid groups had high Rad52 and Rad51 protein expressions (Figure 7(a)). We found no significant difference in Ku80 and Ku70

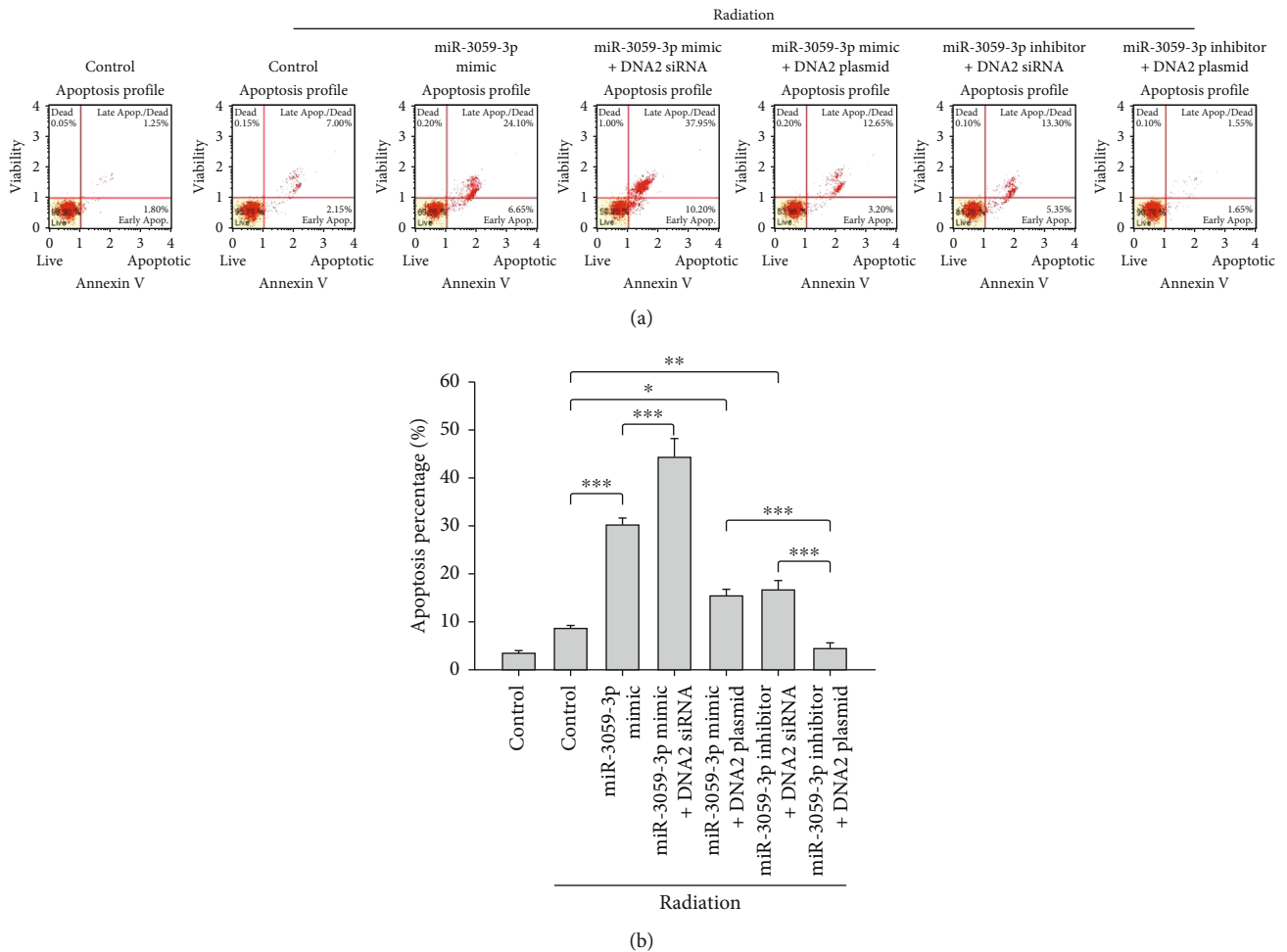


FIGURE 6: Apoptosis assay for miR-3059-3p and DNA2 with radiation. (a) Apoptosis of cells was determined by flow cytometry. (b) The percentage of apoptotic cells. The miR-3059-3p mimic with DNA2 siRNA group showed a higher apoptosis percentage than the other groups. * $P < 0.05$, ** $P < 0.01$, and *** $P < 0.001$.

expressions among the groups (Figures 7(b) and 7(c)). Moreover, in the miR-3059-3p mimic and miR-3059-3p mimic + DNA2 siRNA groups, the intensities of RAD52 and RAD51 were significantly lesser than those in other groups (Figures 7(d) and 7(e)) after radiation exposure. Our findings confirmed the association of miR-3059-3p with RAD52 and RAD51 and that miR-3059-3p increased radiosensitivity by targeting the DNA2 protein to affect the HR pathway in postradiation DNA repair.

4. Discussion

GBM in humans is still the most common primary malignant tumor of the central nervous system. Despite standard treatment including maximal surgical resection and RT with concomitant chemotherapy being well-established, the median progression-free and overall survival after the initial diagnosis is 6.2–7.5 and 14.6–20.5 months, respectively [26]. The main reason for these failures is the development of resistance to standard treatment regimens for GBM, including RR. Most studies over the years have elucidated the

mechanisms of RR of GBM cells, and RR in these cells has been attributed to several mechanisms, including cell cycle, tumor microenvironment, hypoxia, apoptosis, cancer stem cells, microRNAs, and DNA damage and repair. In this study, RR cells exhibited downregulation of miR-3059-3p (Figure 1(a)) and upregulation of DNA2 (Figure 4(b)).

RT often results in DSB in cells. DNA damage response would induce RR in cancer cells. GBM cells develop RR via various DNA repair pathways, such as base excision repair, mismatch repair, nucleotide excision repair, homologous recombination repair, and NHEJ in glioma cells [27–29]. Inhibition of these pathways attenuated the RR cells and subsequent RT efficiency. Specific miRNAs can modulate proteins in the NHEJ pathway in gliomas. Blocking NHEJ-related proteins (KU70/KU80) was able to increase gene targeting efficiency [30].

The RAD51/RAD52 complex plays a key role in the HR pathway. Many studies have shown that inhibition of the HR pathway significantly enhances radiosensitivity in cancer cells. Chandler et al. showed that inhibition of Tat-associated T-cell-derived kinase-induced radiosensitivity

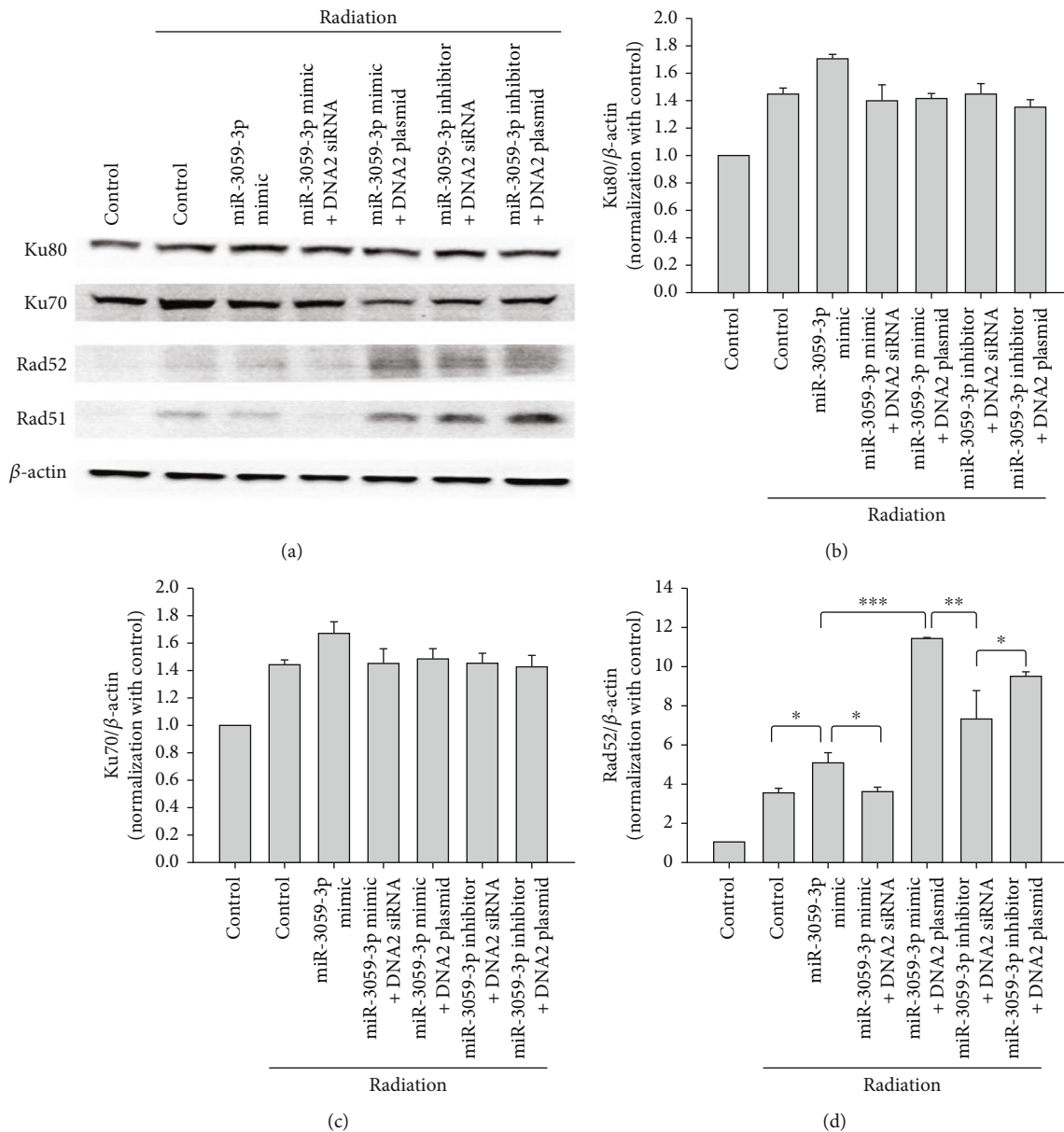
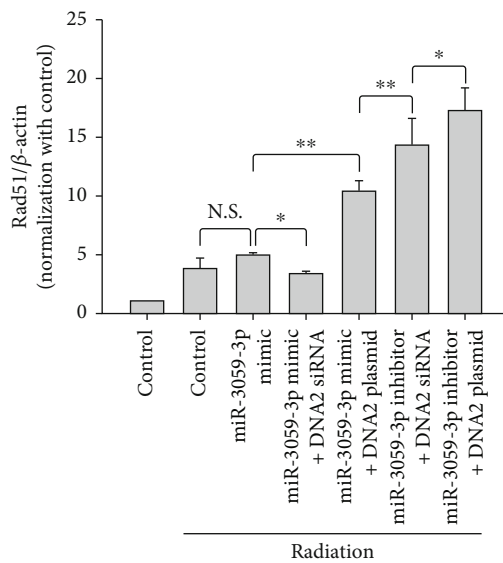


FIGURE 7: Continued.



(e)

FIGURE 7: NHEJ and HR pathways were detected using immunoblotting. (a) Representative results of immunoblotting for Ku80, Ku70, Rad52, and Rad51. The Ku80 (b), Ku70 (c), Rad52 (d), and Rad51 (e) expression levels were normalized control group. * $P < 0.05$, ** $P < 0.01$, and *** $P < 0.001$.

through the HR pathway, not via the NHEJ pathway, in breast cancer [31]. Tang et al. showed that both ATM and EGFR inhibitors promote radiosensitivity through the HR pathway, not via the NHEJ pathway, in lung adenocarcinoma, cervical cancer, GBM, and colorectal carcinoma [32]. Our results revealed that inhibition of the HR pathway, not the NHEJ pathway, via miR-3059-3p enhances the therapeutic effects of radiation.

In this study, we found a relationship between targeting DNA2 protein and RAD51/RAD52 complex and that the DNA2 protein was attenuated via miRNA-3059-3p. DNA2 protein, which was first identified in yeast, plays an important role in DNA replication because of helicase and nuclease activities in the nucleus and mitochondria [33, 34]. DNA2 plays an important role in cell cycle, telomere maintenance, and DNA replication and repair [35]. Increased CHK1 expression has been shown to induce double-strand breaks (DSBs) through phosphorylation of DNA2 [36]. Gupta et al. showed that CHK1 inhibitor hypersensitizes osteosarcoma cells to radiation [37]. In our study, silencing DNA2 through miR-3059-3p targeting increased the percentage of apoptotic cells by inhibiting RAD51/RAD52 expression with radiation in GBM cells.

5. Conclusion

Currently, GBM remains a highly lethal cancer, despite several research efforts and clinical trials with agents designed to improve treatment outcomes. RR is among the reasons of treatment failure and tumor recurrence. Radiosensitizers have been considered and remain a viable option for improving the prognosis in patients with GBM. In our study, we focused on miR-3059-3p to target DNA2 and observed downregulated DNA2 expression. DNA2 plays an essential

role in regulating the HR pathway and initiating DNA repair. Our data suggest that downregulation of DNA2 via miR-3059-3p could attenuate the HR pathway and decrease the possibility of DNA repair. Therefore, we believe that miR-3059-3p is an effective radiosensitizer candidate, which can inhibit GBM recurrence after RT.

Data Availability

Data sharing is not applicable to this article as no datasets were generated or analyzed during the current study.

Conflicts of Interest

The authors declare that they have no conflicts of interests.

Acknowledgments

This study was supported by grants from the Kaohsiung Medical University Hospital (KMUH103-3R18, KMUH104-4R17, KMUH108-8M26, KMUH107-M701, and KMUH109-M908) and Ministry of Science and Technology (110-2314-B-075B-001-MY2).

References

- [1] Q. T. Ostrom, N. Patil, G. Cioffi, K. Waite, C. Kruchko, and J. S. Barnholtz-Sloan, "CBTRUS statistical report: primary brain and other central nervous system tumors diagnosed in the United States in 2013–2017," *Neuro-oncology*, vol. 22, Supplement_1, pp. iv1–iv96, 2020.
- [2] E. Ron, B. Modan, J. D. Boice et al., "Tumors of the brain and nervous system after radiotherapy in childhood," *The New England Journal of Medicine*, vol. 319, no. 16, pp. 1033–1039, 1988.

- [3] Y. Esquenazi, N. Moussazadeh, T. W. Link et al., "Thalamic glioblastoma: clinical presentation, management strategies, and outcomes," *Neurosurgery*, vol. 83, no. 1, pp. 76–85, 2018.
- [4] R. Stupp, W. P. Mason, M. J. van den Bent et al., "Radiotherapy plus concomitant and adjuvant temozolomide for glioblastoma," *The New England Journal of Medicine*, vol. 352, no. 10, pp. 987–996, 2005.
- [5] C. McKinnon, M. Nandhabalan, S. A. Murray, and P. Plaha, "Glioblastoma: clinical presentation, diagnosis, and management," *BMJ*, vol. 14, no. 374, article n1560, 2021.
- [6] Y. Esemien, M. Awan, R. Parwez et al., "Molecular pathogenesis of glioblastoma in adults and future perspectives: a systematic review," *International Journal of Molecular Sciences*, vol. 23, no. 5, p. 2607, 2022.
- [7] Z. Wang, N. P. Peet, P. Zhang, Y. Jiang, and L. Rong, "Current development of glioblastoma therapeutic agents," *Molecular Cancer Therapeutics*, vol. 20, no. 9, pp. 1521–1532, 2021.
- [8] C. Lu-Emerson, D. G. Duda, K. E. Emblem et al., "Lessons from anti-vascular endothelial growth factor and anti-vascular endothelial growth factor receptor trials in patients with glioblastoma," *Journal of Clinical Oncology*, vol. 33, no. 10, pp. 1197–1213, 2015.
- [9] S. E. Combs, T. E. Schmid, P. Vaupel, and G. Multhoff, "Stress response leading to resistance in glioblastoma—the need for innovative radiotherapy (iRT) concepts," *Concepts. Cancers (Basel)*, vol. 8, no. 1, p. 15, 2016.
- [10] E. Stanzani, F. Martínez-Soler, T. M. Mateos et al., "Radioresistance of mesenchymal glioblastoma initiating cells correlates with patient outcome and is associated with activation of inflammatory program," *Oncotarget*, vol. 8, no. 43, pp. 73640–73653, 2017.
- [11] M. J. Tahmasebi-Birgani, A. Teimoori, A. Ghadiri, H. Mansoury-Asl, A. Danyaei, and H. Khanbabaei, "Fractionated radiotherapy might induce epithelial-mesenchymal transition and radioresistance in a cellular context manner," *Journal of Cellular Biochemistry*, vol. 28, 2018.
- [12] D. P. Bartel, "MicroRNAs: genomics, biogenesis, mechanism, and function," *Cell*, vol. 116, no. 2, pp. 281–297, 2004.
- [13] S. Vasudevan, "Posttranscriptional upregulation by microRNAs," *Wiley Interdisciplinary Reviews: RNA*, vol. 3, no. 3, pp. 311–330, 2012.
- [14] J. A. Makarova, M. U. Shkurnikov, D. Wicklein et al., "Intracellular and extracellular microRNA: an update on localization and biological role," *Progress in Histochemistry and Cytochemistry*, vol. 51, no. 3–4, pp. 33–49, 2016.
- [15] M. A. Chaudhry, H. Sachdeva, and R. A. Omaruddin, "Radiation-induced micro-RNA modulation in glioblastoma cells differing in DNA-repair pathways," *DNA and Cell Biology*, vol. 29, no. 9, pp. 553–561, 2010.
- [16] A. Sasaki, Y. Udaka, Y. Tsunoda et al., "Analysis of p53 and miRNA expression after irradiation of glioblastoma cell lines," *Anticancer Research*, vol. 32, no. 11, pp. 4709–4713, 2012.
- [17] A. Besse, J. Sana, P. Fadrus, and O. Slaby, "MicroRNAs involved in chemo- and radioresistance of high-grade gliomas," *Tumour Biology*, vol. 34, no. 4, pp. 1969–1978, 2013.
- [18] Z. Chen, D. Li, Q. Cheng et al., "MicroRNA-203 inhibits the proliferation and invasion of U251 glioblastoma cells by directly targeting PLD2," *Molecular Medicine Reports*, vol. 9, no. 2, pp. 503–508, 2014.
- [19] J. H. Weng, C. C. Yu, Y. C. Lee, C. W. Lin, W. W. Chang, and Y. L. Kuo, "miR-494-3p induces cellular senescence and enhances radiosensitivity in human oral squamous carcinoma cells," *International journal of molecular sciences*, vol. 17, no. 7, p. 1092, 2016.
- [20] X. Yang, M. Li, Y. Zhao, X. Tan, J. Su, and X. Zhong, "Hsa_circ_0079530/AQP4 axis is related to non-small cell lung cancer development and radiosensitivity," *Annals of Thoracic and Cardiovascular Surgery*, vol. oa-21, 2022.
- [21] J. McGrath, L. E. Kane, and S. G. Maher, "The influence of microRNA-31 on oxidative stress and radiosensitivity in pancreatic ductal adenocarcinoma," *Cell*, vol. 11, no. 15, 2022.
- [22] X. Chen, Y. Liu, Q. Zhang et al., "Exosomal miR-590-3p derived from cancer-associated fibroblasts confers radioresistance in colorectal cancer," *Molecular Therapy-Nucleic Acids*, vol. 24, no. 24, pp. 113–126, 2021.
- [23] X. Sun, Z. Song, Y. Si, and J. H. Wang, "MicroRNA and mRNA profiles in ventral tegmental area relevant to stress-induced depression and resilience," *Progress in Neuro-Psychopharmacology & Biological Psychiatry*, vol. 86, no. 86, pp. 150–165, 2018.
- [24] Y. Chen and X. Wang, "miRDB: an online database for prediction of functional microRNA targets," *Nucleic Acids Research*, vol. 48, no. D1, pp. D127–D131, 2020.
- [25] B. B. Kragelund, E. Weterings, R. Hartmann-Petersen, and G. Keijzers, "The Ku70/80 ring in non-homologous end-joining: easy to slip on, hard to remove," *Frontiers in Bioscience-Landmark*, vol. 21, no. 3, pp. 514–527, 2016.
- [26] J. J. Mandel, S. Yust-Katz, A. J. Patel et al., "Inability of positive phase II clinical trials of investigational treatments to subsequently predict positive phase III clinical trials in glioblastoma," *Neuro-Oncology*, vol. 20, no. 1, pp. 113–122, 2018.
- [27] J. A. Schwartzbaum, J. L. Fisher, K. D. Aldape, and M. Wrensch, "Epidemiology and molecular pathology of glioma," *Nature Clinical Practice. Neurology*, vol. 2, no. 9, pp. 494–503, 2006.
- [28] R. Ceccaldi, J. C. Liu, R. Amunugama et al., "Homologous-recombination-deficient tumours are dependent on Pol θ -mediated repair," *Nature*, vol. 518, no. 7538, pp. 258–262, 2015.
- [29] H. H. Y. Chang, N. R. Pannunzio, N. Adachi, and M. R. Lieber, "Non-homologous DNA end joining and alternative pathways to double-strand break repair," *Nature Reviews. Molecular Cell Biology*, vol. 18, no. 8, pp. 495–506, 2017.
- [30] Q. Ji, J. Mai, Y. Ding, Y. Wei, R. Ledesma-Amaro, and X. J. Ji, "Improving the homologous recombination efficiency of *Yarrowia lipolytica* by grafting heterologous component from *Saccharomyces cerevisiae*," *Metabolic engineering communications*, vol. 11, article e00152, 2020.
- [31] B. C. Chandler, L. Moubadder, C. L. Ritter et al., "TTK inhibition radiosensitizes basal-like breast cancer through impaired homologous recombination," *The Journal of Clinical Investigation*, vol. 130, no. 2, pp. 958–973, 2020.
- [32] S. Tang, Z. Li, L. Yang, L. Shen, and Y. Wang, "A potential new role of ATM inhibitor in radiotherapy: suppressing ionizing radiation-activated EGFR," *International Journal of Radiation Biology*, vol. 96, no. 4, pp. 461–468, 2020.
- [33] L. B. Dumas, J. P. Lussky, E. J. McFarland, and J. Shampay, "New temperature-sensitive mutants of *Saccharomyces cerevisiae* affecting DNA replication," *Molecular & General Genetics*, vol. 187, no. 1, pp. 42–46, 1982.
- [34] M. E. Budd and J. L. Campbell, "A yeast replicative helicase, Dna2 helicase, interacts with yeast FEN-1 nuclease in carrying out its essential function," *Molecular and Cellular Biology*, vol. 17, no. 4, pp. 2136–2142, 1997.

- [35] E. Pawlowska, J. Szczepanska, and J. Blasiak, "DNA2-an important player in DNA damage response or just another DNA maintenance protein?," *International Journal of Molecular Sciences*, vol. 18, no. 7, 2017.
- [36] J. M. Enserink and R. D. Kolodner, "An overview of Cdk1-controlled targets and processes," *Cell Division*, vol. 5, no. 1, p. 11, 2010.
- [37] P. Gupta, B. Saha, S. Chattopadhyay, and B. S. Patro, "Pharmacological targeting of differential DNA repair, radio-sensitizes WRN-deficient cancer cells in vitro and in vivo," *Biochemical Pharmacology*, vol. 186, article 114450, 2021.

Research Article

Comparable Clinical Outcome Using Small or Large Gross Tumor Volume-to-Clinical Target Volume Margin Expansion in Neoadjuvant Chemoradiotherapy for Esophageal Squamous Cell Carcinoma

Tae Hoon Lee ¹, Hak Jae Kim ^{1,2,3}, Byoung Hyuck Kim ⁴, Chang Hyun Kang ⁵,
Bhumsuk Keam ⁶, Hyeon Jong Moon ⁷, Yong Won Seong ⁷, and Suzy Kim ^{1,4}

¹Department of Radiation Oncology, Seoul National University Hospital, Seoul, Republic of Korea

²Cancer Research Institute, College of Medicine, Seoul National University, Seoul, Republic of Korea

³Institute of Radiation Medicine, Medical Research Center, Seoul National University, Seoul, Republic of Korea

⁴Department of Radiation Oncology, Seoul Metropolitan Government-Seoul National University Boramae Medical Center, Seoul, Republic of Korea

⁵Department of Thoracic and Cardiovascular Surgery, Seoul National University Hospital, Seoul, Republic of Korea

⁶Department of Internal Medicine, Seoul National University Hospital, Seoul, Republic of Korea

⁷Department of Thoracic and Cardiovascular Surgery,

Seoul Metropolitan Government-Seoul National University Boramae Medical Center, Seoul, Republic of Korea

Correspondence should be addressed to Hak Jae Kim; khjae@snu.ac.kr and Suzy Kim; suzy101@snu.ac.kr

Received 22 March 2022; Accepted 20 May 2022; Published 3 June 2022

Academic Editor: Ya Ju Hsieh

Copyright © 2022 Tae Hoon Lee et al. This is an open access article distributed under the Creative Commons Attribution License, which permits unrestricted use, distribution, and reproduction in any medium, provided the original work is properly cited.

The purpose of this study was to evaluate the feasibility of small primary gross tumor volume (GTV)-to-clinical target volume (CTV) margin expansion in neoadjuvant chemoradiation for esophageal squamous cell carcinoma. Medical records of 139 patients with locally advanced esophageal squamous cell carcinoma who underwent neoadjuvant chemoradiation and radical esophagectomy were retrospectively reviewed. Patients treated with longitudinal primary GTV-to-CTV margin expansion of 2 cm and no additional expansion of the CTV through the esophagus were classified into a small margin (SM) group (37 patients). The remaining 102 patients were classified as a large margin (LM) group. Patterns of recurrence including local and out-field regional recurrence rates were compared between the two groups. Clinical outcomes including rates of local control, regional control, failure-free survival, and overall survival were also compared. More patients in the SM group underwent paclitaxel + carboplatin, McKeown esophagectomy, and intensity-modulated radiation therapy than in the LM group. With a median follow-up of 25.6 months, there was no significant difference in the crude rate of local recurrence (10.8% vs. 6.9%, $P = 0.694$), out-field regional recurrence (27.0% vs. 19.6%, $P = 0.480$), or out-field regional recurrence without in-field recurrence (10.8% vs. 12.7%, $P = 0.988$) between the two groups. There was no significant difference in failure-free survival (5-year, 34.4% vs. 30.6%, $P = 0.652$) or overall survival (44.1% vs. 38.5%, $P = 1.000$), either. Esophageal fistula was not reported in the SM group (0.0% vs. 7.9%, $P = 0.176$). In conclusion, a radiation field with 2 cm of longitudinal primary GTV-to-CTV was feasible in the neoadjuvant setting for esophageal squamous cell carcinoma treatment.

1. Introduction

Trimodality approach including neoadjuvant chemoradiation and surgery has become the standard treatment for

locally advanced esophageal cancer, although the treatment outcome of this approach is still unsatisfactory. For example, the CROSS trial, which established neoadjuvant chemoradiation as a standard, reported a 5-year overall survival

rate of 47% in the neoadjuvant chemoradiation arm [1]. Furthermore, there are concerns about the toxicities of trimodality approach and its impact on oncologic outcomes [2]. Therefore, optimized treatment is needed for better outcomes of locally advanced esophageal cancer. In this perspective, several debates persist regarding the radiotherapy (RT) component of trimodality approach. Field design is one of the discussion focuses for RT. There is a tendency toward a smaller RT field recently. For instance, many centers have implemented involved-field irradiation rather than extensive field including elective supraclavicular fossa or celiac axis nodal irradiation. Although an extensive RT field may decrease recurrences in those nodal areas, the effect of elective field to final treatment outcomes including survival rate is not conclusive [3].

Another important point of debate for RT field design is gross tumor volume (GTV)-to-clinical target volume (CTV) margin expansion for primary esophageal lesion. Traditionally, a 5 cm margin above and below the GTV was recommended to cover subclinical disease [4]. However, a recently published guideline suggested a 3 cm margin for GTV-to-CTV expansion based on pathologic examination of esophagectomy specimens [5, 6]. A previous clinical study also suggested that a 2 cm margin for longitudinal GTV-to-CTV expansion was adequate, showing an acceptable locoregional recurrence rate [7]. As these tendencies toward the smaller field continue, concerns about the safety of these field designs also persist. The purpose of this study was to evaluate the feasibility of small longitudinal primary GTV-to-CTV margin expansion in neoadjuvant chemoradiation for esophageal cancer by comparing patterns of recurrence and oncologic outcomes.

2. Materials and Methods

2.1. Study Population. This study was approved by the institutional review boards of Seoul Metropolitan Government-Seoul National University Boramae Medical Center (IRB no. 30-2021-49) and Seoul National University Hospital (IRB no. H-2105-156-1221) before collecting patient information. Medical records of the patients who underwent neoadjuvant chemoradiation and surgery for locally advanced (T3-4 or N+) esophageal squamous cell carcinoma in two institutions (Seoul Metropolitan Government-Seoul National University Boramae Medical Center and Seoul National University Hospital) from January 2005 to December 2018 were retrospectively reviewed. A total of 188 patients underwent neoadjuvant chemoradiation for esophageal cancer during this period. Seven patients who did not have squamous cell carcinoma histology and nine patients with previous malignancy history in 5 years or concomitant malignancy were excluded. Seven patients who were irradiated less than 40 Gy were also excluded. Among the remaining 165 patients, 26 patients could not undergo radical esophagectomy. As a result, 139 patients were included in the analysis.

2.2. Treatment and Definition of the Groups. Patients underwent simulation computerized tomography (CT) scan in the supine position with both arms abducted and immobilized with wing boards. The primary GTV was defined as an esophageal tumor visualized on CT, positron emission tomography (PET), and endoscopy. Primary CTV was generated with 2.0 to 5.0 cm longitudinal and a 0.5 to 1.0 cm radial margin expansion. If suspected metastatic lymph nodes were confirmed on staging work-up and visible on simulation CT, they were delineated as nodal GTV. Nodal CTV was generated with 0.5 to 1.0 cm margin expansion in all directions. The planning target volume (PTV) was generated by applying 0.5 to 1.0 cm margin around CTVs. Before 2014, RT often consisted of two courses, and reduced-field RT was followed immediately after the first course. In reduced-field RT, primary GTV-to-CTV margin expansion was 0 to 2.0 cm for a longitudinal direction and 0 to 1 cm for a radial direction. The PTV for reduced-field RT was defined as CTV for reduced-field RT with 0 to 1.0 cm margin expansion. Elective RT field in a supraclavicular or celiac axis lymph node area was decided by the treating radiation oncologist. Both three-dimensional conformal radiation therapy (3D-CRT) and intensity-modulated radiation therapy (IMRT) were used. Chemotherapy was administered concurrently with RT, and the regimen was selected by the treating medical oncologist.

After completing chemoradiation, patients underwent radical esophagectomy. Transthoracic esophagectomy was preferred, but the exact surgical method was at the discretion of the treating thoracic surgeon. Adjuvant chemotherapy was administered to the patients with an advanced surgical stage. The patients with positive surgical margin or gross residual disease underwent postoperative RT.

Patients with longitudinal primary GTV-to-CTV margin expansion of 2 cm and no additional longitudinal expansion of the CTV by elective coverage of mediastinum through esophagus beyond initial primary GTV-to-CTV expansion were classified as a small margin (SM) group. Coverage of esophagus within the same axial plane with involved nodal CTV was allowed. Elective irradiation of supraclavicular or celiac axis area was also permitted. As a result, 37 (26.6%) patients were included in the SM group. The remaining 102 patients were classified as a large margin (LM) group. Examples of target delineation of SM group and LM group are illustrated in Figure 1.

2.3. Patterns of Recurrence and Clinical Outcomes. Exact sites of disease recurrence occurring within the follow-up period were categorized into local recurrence, regional recurrence, and distant metastasis. Regional recurrences were further categorized into in-field and out-field recurrences. Disease in paraesophageal and celiac axis lymph node was considered as regional spread, while disease in supraclavicular fossa was considered as distant metastasis, as described in AJCC/UICC staging 8th edition [8, 9]. Crude rates of local recurrence, in-field/out-field regional recurrence, and distant metastasis were compared between the SM and LM groups

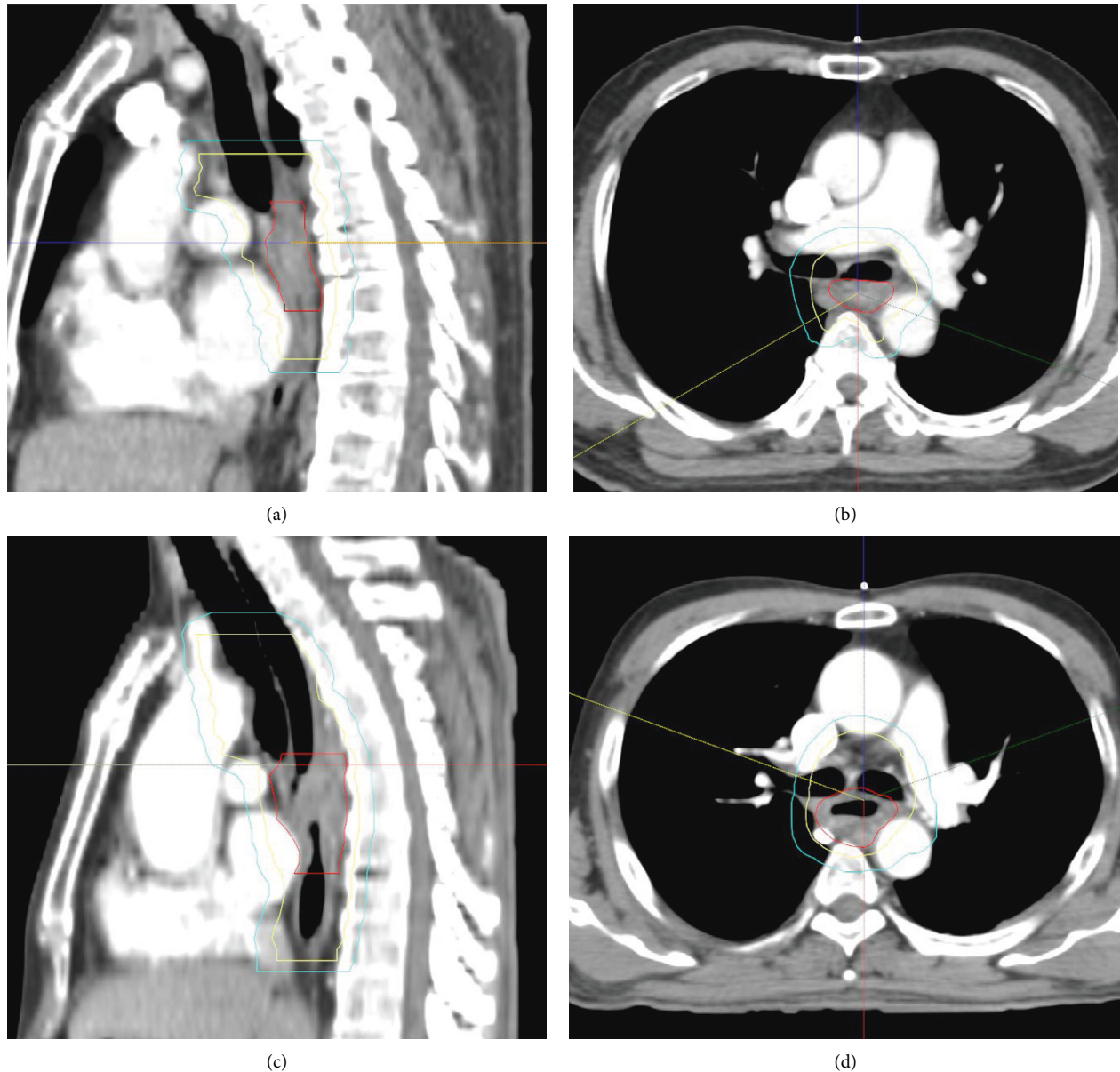


FIGURE 1: Examples of target delineation of small margin (SM) and large margin (LM) groups. Red, yellow, and cyan lines indicate gross tumor volume (GTV), clinical target volume (CTV), and planning target volume (PTV), respectively. (a) Sagittal and (b) axial cuts from the representative case of the SM group illustrating target delineation with longitudinal primary GTV-to-CTV of 2 cm and no additional elective field for the longitudinal direction. (c) Sagittal and (d) axial cuts of representative case from the LM group illustrating target delineation with more extensive CTV, especially in the longitudinal direction.

by chi-square test. Locations of distant metastasis were also compared between two groups by chi-square test.

Rates of local control (LC), regional control (RC), failure-free survival (FFS), and overall survival (OS) were calculated using the Kaplan–Meier method. An LC event was defined as recurrence of disease in the anastomotic site and an RC event was defined as recurrence of disease in the mediastinal and celiac axis lymph node area. An FFS event was defined as any failure or death, while an OS event was defined as the death of a patient from any cause. Survival data were retrieved from the resident registration system of the government of the Republic of Korea. LC, RC, FFS, and

OS of two groups were compared by log-rank test. Univariate analysis was performed for LC, RC, FFS, and OS to identify potential preoperative prognostic factors affecting treatment outcomes. Statistically significant or marginally significant variables ($P < 0.1$) and RT field (SM vs. LM group) were incorporated into the multivariate analysis using the Cox proportional hazards model to investigate the effect of RT field and other potential variables on the clinical outcomes. Rates of major toxicities including esophageal stricture requiring intervention and fistula were calculated and compared by chi-square test between the two groups. P value less than 0.05 was defined as statistically significant

TABLE 1: Patient characteristics.

Characteristics	Small margin group (N= 37)	Large margin group (N= 102)	P value
Age (years, median, range)	61.5 (39.2–76.7)	62.4 (35.2–81.6)	0.567
Sex			0.760
Male	34 (91.9%)	97 (95.1%)	
Female	3 (8.1%)	5 (4.9%)	
ECOG performance status			0.625
0	8 (21.6%)	15 (14.7%)	
1	28 (75.7%)	84 (82.4%)	
2	1 (2.7%)	3 (2.9%)	
Differentiation (prechemoradiation)			0.795*
Well differentiated	2 (5.4%)	9 (8.8%)	
Moderately differentiated	27 (73.0%)	73 (71.6%)	
Poorly differentiated	3 (8.1%)	10 (9.8%)	
Unknown	5 (13.5%)	10 (9.8%)	
Subsite			0.008
Upper thoracic	13 (35.1%)	13 (12.7%)	
Upper and middle thoracic	5 (13.5%)	5 (4.9%)	
Middle thoracic	6 (16.2%)	26 (25.5%)	
Middle and lower thoracic	2 (5.4%)	11 (10.8%)	
Lower thoracic	11 (29.7%)	47 (46.1%)	
Clinical T stage			0.801*
cT1	2 (5.4%)	4 (3.9%)	
cT2	7 (18.9%)	26 (25.5%)	
cT3	27 (73.0%)	66 (64.7%)	
cT4	1 (2.7%)	4 (3.9%)	
Unknown	0 (0.0%)	2 (2.0%)	
Clinical N stage			0.012
cN0	7 (18.9%)	16 (15.7%)	
cN1	16 (43.2%)	68 (66.7%)	
cN2	12 (32.4%)	18 (17.6%)	
cN3	2 (5.4%)	0 (0.0%)	
Clinical M stage			0.400
cM0	27 (73.0%)	83 (81.4%)	
cM1	10 (27.0%)	19 (18.6%)	
Chemotherapy regimen			0.003
5-FU + cisplatin	6 (16.2%)	45 (44.1%)	
Paclitaxel + carboplatin	29 (78.4%)	47 (46.1%)	
Others	2 (5.4%)	10 (9.8%)	
Chemotherapy completed			0.527
Yes	35 (94.6%)	91 (89.2%)	
No	2 (5.4%)	11 (10.8%)	
Radiotherapy technique			0.029
3D-CRT	21 (56.8%)	79 (77.5%)	
IMRT	16 (43.2%)	23 (22.5%)	
Total radiation dose			0.001
<50.4 Gy	34 (91.9%)	62 (60.8%)	
≥50.4 Gy	3 (8.1%)	40 (39.2%)	
Supraclavicular elective irradiation			1.000
Yes	8 (21.6%)	22 (21.6%)	
No	29 (78.4%)	80 (78.4%)	
Longitudinal length of primary GTV (cm, mean ± SD)	5.8 ± 1.9	6.5 ± 3.1	0.112
CTV (cm ³ , mean ± SD)	179.4 ± 67.0	222.6 ± 81.5	0.005
PTV (cm ³ , mean ± SD)	419.0 ± 120.6	501.3 ± 150.4	0.003
Type of surgery			0.001
Mckeown	31 (83.8%)	50 (49.0%)	
Ivor–Lewis	6 (16.2%)	51 (50.0%)	
Transhiatal	0 (0.0%)	1 (1.0%)	
Lymph node dissection			<0.001*
2-field	5 (13.5%)	53 (52.0%)	
3-field	32 (86.5%)	45 (44.1%)	
Unknown	0 (0.0%)	4 (3.9%)	

TABLE 1: Continued.

Characteristics	Small margin group (N= 37)	Large margin group (N= 102)	P value
Number of lymph nodes harvested (median, range)	53 (16–93)	45 (5–113)	0.218
Margin status			0.527
R0	36 (97.3%)	94 (92.2%)	
R1	1 (2.7%)	8 (7.8%)	
Pathologic complete resolution			0.880
Yes	9 (24.3%)	28 (27.5%)	
No	28 (75.7%)	74 (72.5%)	
Postoperative radiotherapy			0.392
Yes	0 (0.0%)	5 (4.9%)	
No	37 (100.0%)	97 (95.1%)	
Adjuvant chemotherapy			0.955
Yes	7 (18.9%)	17 (16.7%)	
No	30 (81.1%)	85 (83.3%)	

*The patients with unknown value were excluded from the calculation of this *P* value. Abbreviations: ECOG, Eastern Cooperative Oncology Group; 5-FU, 5-fluorouracil; 3D-CRT, 3-dimensional conformal radiation therapy; IMRT, intensity-modulated radiation therapy; GTV, gross tumor volume; CTV, clinical target volume; PTV, planning target volume.

throughout all statistical tests. All statistical analyses were performed using R 4.1.1 (The R Foundation for Statistical Computing, Vienna, Austria).

3. Results

3.1. Patient Characteristics. Patient characteristics are summarized in Table 1. A median follow-up period was 25.6 months (range, 3.0 to 141.5 months) for all patients and 58.3 months (range, 19.5 to 129.7 months) for surviving patients only. Total cumulative prescribed radiation dose had a median of 45 Gy (range, 40 to 54 Gy). Dose per fraction was 1.8 Gy for most (95%) patients. Six (4.3%) patients had dose per fraction of 2 Gy. One (0.7%) patient had 2.25 Gy per fraction. Reduced-field RT was conducted in 44 (31.6%) patients. The prescribed dose of reduced-field RT was 5.4 Gy (range, 3.6 to 9.0 Gy) except for three patients. Total cumulative RT dose was lower in the SM group than in the LM group due to less usage of reduced-field irradiation. All but one patient who was irradiated less than 50.4 Gy did not have a reduced-field irradiation, while patients irradiated ≥ 50.4 Gy had reduced-field irradiation. 3D-CRT was applied for RT planning in 100 (71.9%) patients. The remaining 39 (28.1%) patients used IMRT. Thirty (29.1%) patients underwent supraclavicular elective irradiation. No patient received elective irradiation in the celiac axis lymph node area. In the LM group, a median actual longitudinal distance between the primary GTV and the superior margin of the CTV covering the esophagus was 5.6 cm (range, 2.0 to 16.2 cm), and a median distance between the primary GTV and the inferior margin of the CTV was 2.0 cm (range, 2.0 to 7.8 cm). The distance between the primary GTV and the superior margin of the CTV was longer because upper mediastinal elective CTV was frequently set by the treating radiation oncologist, while GTV-to-CTV expansion to an inferior direction was often limited by the gastroesophageal junction.

Regarding concurrent chemotherapy, weekly paclitaxel + carboplatin was applied to 76 (54.7%) patients and 5-fluorouracil (5-FU) + cisplatin was applied to 51 (36.7%)

patients. Weekly cisplatin was administered to 10 (7.2%) patients. Cetuximab + paclitaxel + carboplatin and docetaxel + cisplatin were used in one (0.7%) patient each. There was a significantly increased use of weekly paclitaxel + carboplatin after 2014 (before 2014, 21.3% vs. after 2014, 80.8%, $P < 0.001$). Planned chemotherapy was completely administered to 126 (90.6%) patients.

Almost all (99.3%) of patients underwent transthoracic esophagectomy, and one (0.7%) patient underwent transhiatal esophagectomy. Among patients who underwent transthoracic esophagectomy, Mckeown esophagectomy was applied to 81 (58.3%) patients, and Ivor–Lewis esophagectomy was applied to 57 (41.0%) patients. Regarding lymph node dissection, 77 (55.4%) patients underwent a 3-field dissection and 58 (41.7%) patients underwent a 2-field dissection. Four (2.9%) patients had no information about the type of lymph node dissection. Median interval between the end of chemoradiation and surgery was 42 days (range, 23 to 95 days). Adjuvant chemotherapy was administered to 24 (17.3%) patients. The regimen of adjuvant chemotherapy was 5-FU + cisplatin for 20 patients and docetaxel + cisplatin for three patients. One patient went to another institution for adjuvant chemotherapy with an unknown regimen. Five (3.6%) patients with R1 resection underwent postoperative RT to the esophageal tumor bed, and the median dose was 16.2 Gy (range, 14.4 to 20.0 Gy).

There were some differences in treatment between the SM and LM group mainly due to changes in dominant treatment method by period. In the SM group, 21 (56.8%) patients started chemoradiation in 2017 and 2018, while in the LM group, 20 (19.6%) patients started chemoradiation in the same period. More patients in the SM group underwent paclitaxel + carboplatin as a chemotherapeutic regimen (78.4% vs. 46.1%), IMRT for RT planning (43.2% vs. 22.5%), Mckeown esophagectomy (83.8% vs. 49.0%), and 3-field lymph node dissection (86.5% vs. 44.1%) than in the LM group. Median number of dissected lymph nodes was 47 (range, 5 to 113) in the entire cohort. No increase in R1 resection was observed in the SM group (2.7% vs. 7.8%).

In addition, the SM group had more N2/3 disease (37.8% vs. 17.6%). Patients in the SM group had more upper esophageal (above azygos vein) involvement (48.6% vs. 17.6%) but less lower esophageal (below inferior pulmonary vein) involvement (35.1% vs. 56.9%). This was due to a tendency to extend the CTV to the upper mediastinal lymph node area in the nonupper esophageal primary lesion, resulting in an inclusion of part of upper esophagus in the CTV, which made the patient ineligible to be classified into the SM group.

Twenty-nine (28.4%) patients with clinical M1 disease were included in this study. Twenty-two patients (8 from the SM group and 14 from the LM group) had distant metastasis in the supraclavicular lymph node only and 2 patients (one from the SM group and one from the LM group) had abdominal para-aortic lymph node metastasis. Four patients (one from the SM group and 3 from the LM group) had neck lymph node metastasis at the time of diagnosis. One patient in the LM group had lung metastasis, which was histologically confirmed before chemoradiation. The lung tumor was regressed during chemoradiation. The patient underwent metastasectomy and radical esophagectomy.

3.2. Patterns of Recurrence. Patterns of recurrence occurring during the follow-up period are summarized in Table 2. No significant difference between the two groups was observed for each failure site. There was no difference in the crude rate of local recurrence (10.8% vs. 6.9%, $P = 0.684$), all out-field regional recurrence (27.0% vs. 19.6%, $P = 0.480$), or crude rate of isolated out-field regional recurrence without in-field recurrence (10.8% vs. 12.7%, $P = 0.988$) between SM and LM groups. The most frequent site of distant metastasis was lung. Forty (28.8%) patients had lung metastasis during the follow-up period. Metastases to nonregional lymph nodes (27 patients, 19.4%) and liver (20 patients, 14.4%) were also frequent. Sites of distant metastasis showed no difference between the two groups. One (2.7%) patient in the SM group and four (3.9%) patients in the LM group had celiac axis lymph node failure ($P = 1.000$). There was no significant difference in the crude rate of supraclavicular lymph node failure between the two groups (8.1% vs. 15.7%, $P = 0.384$).

3.3. Clinical Outcomes. The Kaplan–Meier curves of LC, RC, FFS, and OS are illustrated in Figure 2. Three-year and 5-year LC rates were 85.7% and 85.7% in the SM group and 89.6% and 89.6% in the LM group, respectively. Three-year and 5-year RC rates were 68.1% and 59.6% in the SM group and 62.5% and 58.7% in the LM group, respectively. There were no significant differences in LC ($P = 0.444$) or RC ($P = 0.784$) rates between the two groups. Three-year and 5-year FFS rates were 42.9% and 34.4% in the SM group and 39.0% and 30.6% in the LM group, respectively. Three-year and 5-year OS rates were 48.1% and 44.1% in the SM group and 48.6% and 38.5% in the LM group, respectively. There was no significant difference in FFS ($P = 0.652$) or OS ($P = 1.000$) between the two groups.

Results of univariate and multivariate analyses for clinical outcomes are summarized in Supplementary Table 1

and Table 3, respectively. Completeness of chemotherapy was associated with better LC in univariate analysis. In a multivariate model with RT field (SM vs. LM group), this significant association was maintained, while field size was not associated with LC. No variables showed association with RC. Age, supraclavicular elective irradiation, and longitudinal length of GTV were associated with FFS in univariate analysis. In multivariate analysis, older age and longer longitudinal length of GTV were associated with worse FFS. Age, upper thoracic involvement, supraclavicular elective irradiation, and longitudinal length of GTV were associated with OS in univariate analysis. In multivariate analysis, older age and longer longitudinal length of GTV were associated with worse OS. RT field was not associated with FFS or OS in multivariate models.

Regarding major toxicities, four (10.8%) patients from the SM group and 19 (18.8%) patients from the LM group had esophageal stricture requiring intervention. Eight (7.9%) patients from the LM group had esophageal fistula, although no patient from the SM group had such event. Overall, four (10.8%) patients from the SM group and 24 (23.8%) patients from the LM group had either stricture or fistula. These toxicity rates were not significantly different between the two groups (stricture, $P = 0.390$; fistula, $P = 0.176$; stricture or fistula, $P = 0.151$).

4. Discussion

The current study investigated the effect of using the RT field of small or large primary GTV-to-CTV margin expansion on the failure patterns and clinical outcomes in neoadjuvant chemoradiotherapy for esophageal squamous cell carcinoma and showed that small longitudinal primary GTV-to-CTV margin expansion did not significantly harm the treatment outcomes of esophageal squamous cell carcinoma.

Implementing a small RT field in our group was a result of multidisciplinary discussion, especially between thoracic surgeons and radiation oncologists. Several studies have shown that a higher number of lymph node dissected resulted in better treatment outcomes [10, 11], thus favoring extensive lymph node dissection, although this concept is challenged by reports published after the implementation of neoadjuvant chemoradiation [12]. Even after publications of randomized evidence, several groups of surgeons mainly from East Asia have emphasized the importance of extensive lymph node dissection [13, 14]. As easily assumed from the median number of removed lymph nodes in this cohort, which is close to 50, thoracic surgeons in our institutions also support extensive lymphadenectomy. Major concerns of these surgeons about neoadjuvant treatment are technical difficulties of surgical approach to the mediastinum due to fibrosis and adhesion caused by radiation, which might impact postoperative morbidities and mortalities [15, 16]. Thoracic surgeons in our institution constantly suggested to move toward smaller RT fields. As reports about the feasibility of involved-field irradiation for esophageal squamous cell carcinoma of Asian population are accumulated [17, 18] and smaller longitudinal primary GTV-to-CTV margin expansion than the traditional RT field was applied,

TABLE 2: Patterns of recurrence.

Site of recurrence	Small margin group (N = 37)	Large margin group (N = 102)	P value
Any recurrence	18 (48.6%)	56 (54.9%)	0.645
Local recurrence	4 (10.8%)	7 (6.9%)	0.684
Regional recurrence	11 (29.7%)	35 (34.3%)	0.761
In-field recurrence	7 (18.9%)	22 (21.6%)	0.917
In-field recurrence without out-field recurrence	1 (2.7%)	15 (14.7%)	0.097
Out-field recurrence	10 (27.0%)	20 (19.6%)	0.480
Out-field recurrence without in-field recurrence	4 (10.8%)	13 (12.7%)	0.988
In-field and out-field recurrences	6 (16.2%)	7 (6.9%)	0.179
Distant metastasis	16 (43.2%)	51 (50.0%)	0.608
Lung	10 (27.0%)	30 (29.4%)	0.950
Nonregional lymph node	5 (13.5%)	22 (21.6%)	0.413
Supraclavicular fossa	3 (8.1%)	16 (15.7%)	0.384
Neck	2 (5.4%)	9 (8.8%)	0.761
Intra-abdominal	2 (5.4%)	9 (8.8%)	0.761
Axilla	2 (5.4%)	1 (1.0%)	0.354
Liver	4 (10.8%)	16 (15.7%)	0.652
Bone	2 (5.4%)	12 (11.8%)	0.434
Pleural seeding	2 (5.4%)	8 (7.8%)	0.904
Others	5 [†] (13.5%)	13 [‡] (12.7%)	1.000

[†]Adrenal gland = 2, kidney = 2, and hypopharynx = 1. [‡]Peritoneal seeding = 5, adrenal gland = 3, kidney = 3, pancreas = 2, hypopharynx = 1, brain = 1, cecum = 1, and psoas muscle = 1. One patient had both peritoneal seeding and pancreatic metastasis, and another patient had both adrenal and cecal metastasis. One patient had peritoneal, renal, and psoas muscle metastasis.

radiation oncologists of our institutions also start to favor smaller RT fields.

Even with the trend toward smaller fields, 2 cm of longitudinal primary GTV-to-CTV margin is smaller than the lower limit of generally accepted margin expansion. Many radiation oncologists are reluctant to reduce longitudinal primary GTV-to-CTV margin to be smaller than 3 cm based on pathological and clinical data [6, 7]. Furthermore, there is a report that the residual tumor after neoadjuvant chemoradiation might have a devastating effect on survival rate [19]. However, the clinical outcomes of SM group were not inferior to that of LM group in the current study, which included East Asian esophageal squamous cell carcinoma patients with a relatively advanced clinical stage. Recently, our group has implemented involved-field irradiation for neoadjuvant chemoradiation for esophageal cancer. We are waiting for maturation of patient cohort with a small primary GTV-to-CTV margin and strict involved-field irradiation, which does not have additional RT field outside of initially generated primary and nodal CTV by margin expansion, for further reduction of RT field.

The current study reported that 33.1% of all patients experienced regional recurrence. This rate is relatively higher than the locoregional recurrence rate of around 20% from the prospective series that applied neoadjuvant chemoradiation [1, 20–22]. When interpreting recurrence patterns of esophageal cancer, the histological difference needs to be considered. It is acknowledged that squamous cell carcinoma has a tendency to have more locoregional recurrence, while adenocarcinoma has a tendency to have more distant metastasis [23, 24]. The patient cohort of the current study consisted of squamous cell carcinoma only, which is dominant in the East Asian population. Baseline characteristics of the patients also should be taken into account.

Only 15 patients (10.8%) of the cohort had diseases confined to the esophagus, and a high percentage of the patients had regional and nonregional lymph node metastasis. Furthermore, the 7th edition AJCC/UICC system defines any paraesophageal lymph nodes from cervical nodes to celiac nodes as regional lymph nodes regardless of location of primary lesion within esophagus, which is broader than the definition from the previous edition [25]. Some prior reports used the 6th edition of AJCC/UICC system. The rate of regional recurrence might be higher in the current study even with a similar recurrence pattern when compared with these reports.

In this current study, major toxicities including esophageal stricture that required intervention and fistula were reported. Being a retrospective study, minor toxicities were not well-documented and thus were not included in the analysis. Reported rates of major toxicities were lower in the SM group and no patient in the SM group had esophageal fistula, although the differences of these rates did not reach statistical significance. It is well known that the RT field may impact toxicity rates [16, 18]. Smaller RT field might be beneficial to lower surgical morbidities. This should be addressed in further studies with a larger cohort.

It is hard to conclude the impact of different chemotherapeutic regimens of chemoradiotherapy on the clinical outcomes. Conflicting results of comparison studies between paclitaxel + carboplatin and 5-FU + cisplatin have been reported [26, 27]. In the current study, no difference in treatment outcomes by chemotherapeutic regimen was observed, but incomplete chemotherapy was associated with lower LC. Additional research on optimal combination of chemotherapy regimens is needed in the future.

Statistically significant prognostic factors for FFS and OS in the current study were age and longitudinal length of

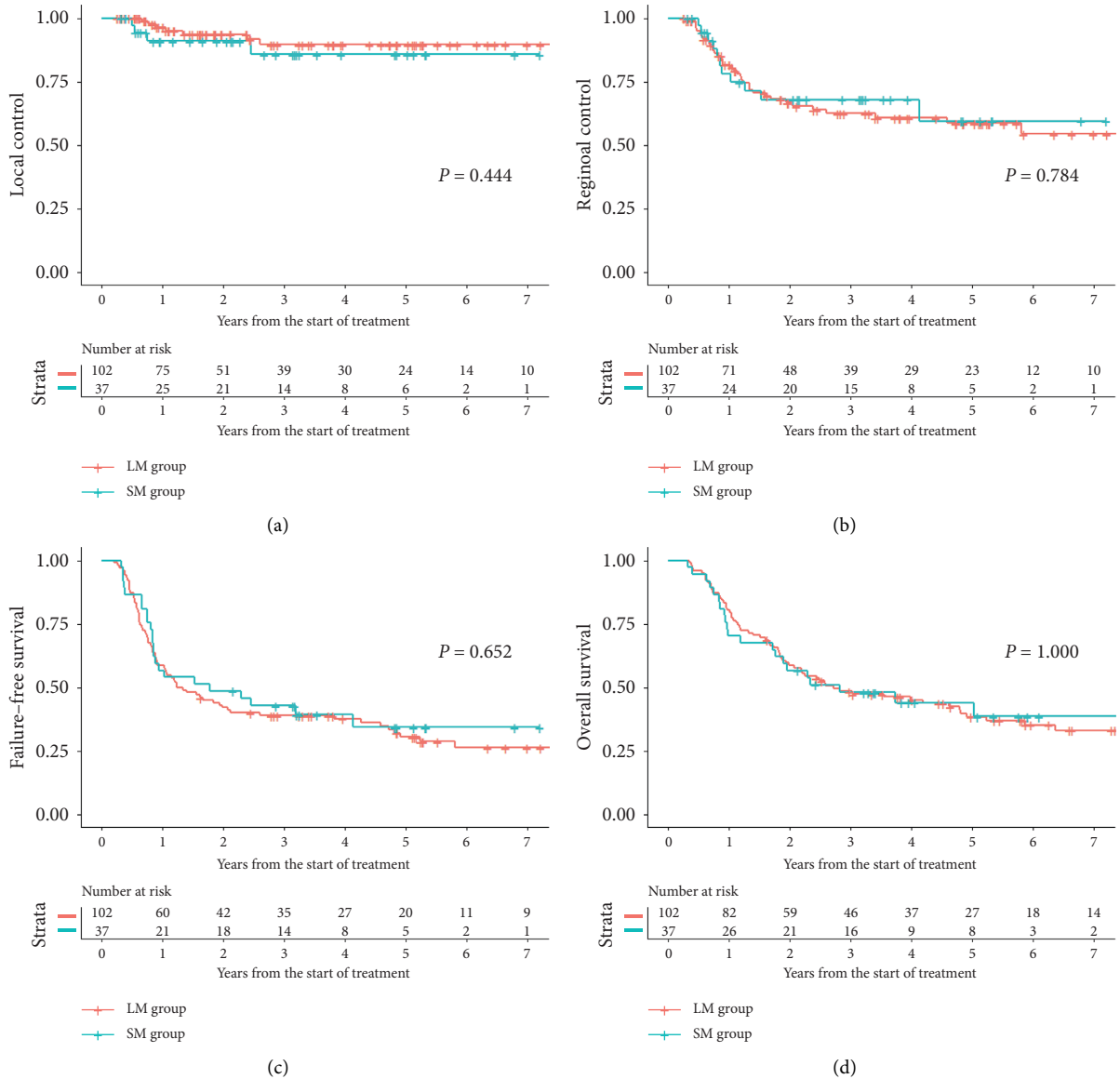


FIGURE 2: Kaplan-Meier curves of (a) local control, (b) regional control, (c) failure-free survival, and (d) overall survival.

TABLE 3: Multivariate analysis of clinical outcomes.

Characteristics (comparison vs. reference)	Local control			Failure-free survival			Overall survival		
	HR	95% CI	P value	HR	95% CI	P value	HR	95% CI	P value
Age (continuous)	—	—	—	1.033	1.006–1.061	0.018	1.041	1.011–1.072	0.007
Upper thoracic involvement (yes vs. no)	—	—	—	—	—	—	0.759	0.398–1.445	0.401
Supraclavicular elective irradiation (yes vs. no)	—	—	—	0.671	0.382–1.180	0.166	0.798	0.399–1.593	0.522
Longitudinal length of primary GTV (continuous)	—	—	—	1.106	1.031–1.186	0.005	1.093	1.017–1.174	0.016
Chemotherapy completed (yes vs. no)	0.160	0.046–0.563	0.004	—	—	—	—	—	—
Field size (small margin vs. large margin group)	1.997	0.571–6.980	0.279	1.057	0.650–1.718	0.824	1.268	0.745–2.157	0.382

Abbreviations: HR, hazard ratio; CI, confidence interval; GTV, gross tumor volume.

primary GTV. The length of primary lesion is a well-known risk factor for survival [28]. We used the length of primary GTV instead due to the lack of endoscopic description for the length of esophageal lesion. Our result was concordant with previous studies using the length measured from

staging work-ups. Other differences in treatment such as RT technique (3D-CRT vs. IMRT) and type of surgical approach did not lead to significant differences in the treatment outcomes. This might be due to the lack of statistical power, and further studies are needed to clarify this.

This study has several limitations. First, the effect of RT field was hard to isolate due to the retrospective nature of this study. Several differences of patient characteristics and treatment factors were observed between the two groups, although univariate and multivariate analyses did not show any evidence of worse clinical outcomes for the SM group. Further studies with more comparable or prospective cohorts would be warranted. Second, principles for target volume delineation were gradually changed, and this might have mitigated potential differences in outcomes between the two groups. Third, the patient selection factor should be considered. Additional RT field in the mediastinum was applied in discretion of the treating radiation oncologist and patients with a high risk of mediastinal lymph node metastasis were most likely to be implemented additional mediastinal RT field encompassing both lymph node area and esophagus, which made the patient ineligible for being classified into the SM group. Nevertheless, the current study showed that limited primary GTV-to-CTV margin expansion resulted in comparable clinical outcomes and patterns of failure, contrary to concerns from some radiation oncologists.

In conclusion, 2 cm of longitudinal primary GTV-to-CTV margin expansion is feasible for neoadjuvant chemoradiation for locally advanced esophageal squamous cell carcinoma. Although not reaching statistical significance, no patient in the SM group had an esophageal fistula. Caution would be needed when applying this principle as target volume delineation should be tailored by each institution with interdepartmental discussion. A further study applying both small margin and involved-field irradiation is underway.

Data Availability

Research data are stored in an institutional repository and will be shared upon request to the corresponding author.

Conflicts of Interest

The authors declare that they have no conflicts of interest.

Supplementary Materials

Supplementary Table 1. Univariate analysis of clinical outcomes. (*Supplementary Materials*)

References

- [1] J. Shapiro, J. J. B. van Lanschot, M. C. C. M. Hulshof et al., "Neoadjuvant chemoradiotherapy plus surgery versus surgery alone for oesophageal or junctional cancer (CROSS): long-term results of a randomised controlled trial," *The Lancet Oncology*, vol. 16, no. 9, pp. 1090–1098, 2015.
- [2] W. B. Robb, M. Messenger, M. C. Gronnier et al., "High-grade toxicity to neoadjuvant treatment for upper gastrointestinal carcinomas: what is the impact on perioperative and oncologic outcomes?" *Annals of Surgical Oncology*, vol. 22, no. 11, pp. 3632–3639, 2015.
- [3] F. M. Hsu, J. M. Lee, P. M. Huang et al., "Retrospective analysis of outcome differences in preoperative concurrent chemoradiation with or without elective nodal irradiation for esophageal squamous cell carcinoma," *International Journal of Radiation Oncology, Biology, Physics*, vol. 81, no. 4, pp. e593–e599, 2011.
- [4] E. C. Halperin, D. E. Wazer, C. A. Perez, and L. W. Brady, *Principles and Practice of Radiation Oncology*, Wolters Kluwer, Alphen aan den Rijn, Netherlands, 7th edition, 2018.
- [5] M. Thomas, H. R. Mortensen, L. Hoffmann et al., "Proposal for the delineation of neoadjuvant target volumes in oesophageal cancer," *Radiotherapy & Oncology*, vol. 156, pp. 102–112, 2021.
- [6] X.-S. Gao, X. Qiao, F. Wu et al., "Pathological analysis of clinical target volume margin for radiotherapy in patients with esophageal and gastroesophageal junction carcinoma," *International Journal of Radiation Oncology, Biology, Physics*, vol. 67, no. 2, pp. 389–396, 2007.
- [7] M. R. Button, C. A. Morgan, E. S. Croydon, S. A. Roberts, and T. D. L. Crosby, "Study to determine adequate margins in radiotherapy planning for esophageal carcinoma by detailing patterns of recurrence after definitive chemoradiotherapy," *International Journal of Radiation Oncology, Biology, Physics*, vol. 73, no. 3, pp. 818–823, 2009.
- [8] S. Edge, D. R. Byrd, A. Trotti, A. G. Fritz, C. C. Compton, and F. L. Greene, *American Joint Committee on Cancer (AJCC) Cancer Staging Manual*, Springer, Berlin, Germany, 8th edition, 2017.
- [9] W.-P. Wang, S.-L. He, Y.-S. Yang, and L.-Q. Chen, "Strategies of nodal staging of the TNM system for esophageal cancer," *Annals of Translational Medicine*, vol. 6, no. 4, p. 77, 2018.
- [10] S. S. Groth, B. A. Virnig, B. A. Whitson et al., "Determination of the minimum number of lymph nodes to examine to maximize survival in patients with esophageal carcinoma: data from the surveillance epidemiology and end results database," *The Journal of Thoracic and Cardiovascular Surgery*, vol. 139, no. 3, pp. 612–620, 2010.
- [11] N. P. Rizk, H. Ishwaran, T. W. Rice et al., "Optimum lymphadenectomy for esophageal cancer," *Annals of Surgery*, vol. 251, no. 1, pp. 46–50, 2010.
- [12] A. Koen Talsma, J. Shapiro, C. W. N. Looman et al., "Lymph node retrieval during esophagectomy with and without neoadjuvant chemoradiotherapy," *Annals of Surgery*, vol. 260, no. 5, pp. 786–793, 2014.
- [13] S. Y. Kim, S. Park, I. K. Park, Y. T. Kim, and C. H. Kang, "Lymph node status after neoadjuvant chemoradiation therapy for esophageal cancer according to radiation field coverage," *The Korean Journal of Thoracic and Cardiovascular Surgery*, vol. 52, no. 5, pp. 353–359, 2019.
- [14] H. Udagawa, "Past, present, and future of three-field lymphadenectomy for thoracic esophageal cancer," *Annals of Gastroenterological Surgery*, vol. 4, no. 4, pp. 324–330, 2020.
- [15] Y. Nabeya, T. Ochiai, H. Matsubara et al., "Neoadjuvant chemoradiotherapy followed by esophagectomy for initially resectable squamous cell carcinoma of the esophagus with multiple lymph node metastasis," *Diseases of the Esophagus*, vol. 18, no. 6, pp. 388–397, 2005.
- [16] A. Juloori, S. L. Tucker, R. Komaki et al., "Influence of preoperative radiation field on postoperative leak rates in esophageal cancer patients after trimodality therapy," *Journal of Thoracic Oncology*, vol. 9, no. 4, pp. 534–540, 2014.
- [17] X. Zhang, M. Li, X. Meng et al., "Involved-field irradiation in definitive chemoradiotherapy for locally advanced esophageal squamous cell carcinoma," *Radiation Oncology*, vol. 9, no. 1, pp. 64–67, 2014.

- [18] Y.-J. Cheng, S.-W. Jing, L.-L. Zhu et al., "Comparison of elective nodal irradiation and involved-field irradiation in esophageal squamous cell carcinoma: a meta-analysis," *Journal of Radiation Research*, vol. 59, no. 5, pp. 604–615, 2018.
- [19] C. Muijs, J. Smit, A. Karrenbeld et al., "Residual tumor after neoadjuvant chemoradiation outside the radiation therapy target volume: a new prognostic factor for survival in esophageal cancer," *International Journal of Radiation Oncology, Biology, Physics*, vol. 88, no. 4, pp. 845–852, 2014.
- [20] M. Stahl, M. K. Walz, J. Riera-Knorrenschild et al., "Preoperative chemotherapy versus chemoradiotherapy in locally advanced adenocarcinomas of the oesophagogastric junction (POET): long-term results of a controlled randomised trial," *European Journal of Cancer*, vol. 81, pp. 183–190, 2017.
- [21] G. A. von Döbeln, F. Klevebro, A. B. Jacobsen et al., "Neoadjuvant chemotherapy versus neoadjuvant chemoradiotherapy for cancer of the esophagus or gastroesophageal junction: long-term results of a randomized clinical trial," *Diseases of the Esophagus*, vol. 32, no. 2, pp. 1–11, 2019.
- [22] S. Liu, J. Wen, H. Yang et al., "Recurrence patterns after neoadjuvant chemoradiotherapy compared with surgery alone in oesophageal squamous cell carcinoma: results from the multicenter phase III trial NEOCRTEC5010," *European Journal of Cancer*, vol. 138, no. 651, pp. 113–121, 2020.
- [23] M. Xi, Y. Yang, L. Zhang et al., "Multi-institutional analysis of recurrence and survival after neoadjuvant chemoradiotherapy of esophageal cancer," *Annals of Surgery*, vol. 269, no. 4, pp. 663–670, 2019.
- [24] A. Barbetta, S. T. Nobel, M. Hsu et al., "Patterns and risk of recurrence in patients with esophageal cancer with a pathologic complete response after chemoradiotherapy followed by surgery," *The Journal of Thoracic and Cardiovascular Surgery*, vol. 157, no. 3, 2019.
- [25] T. W. Rice, E. H. Blackstone, and V. W. Rusch, "7th edition of the AJCC cancer staging manual: esophagus and esophagogastric junction," *Annals of Surgical Oncology*, vol. 17, no. 7, pp. 1721–1724, 2010.
- [26] K. R. Haisley, K. D. Hart, N. Nabavizadeh et al., "Neoadjuvant chemoradiotherapy with concurrent cisplatin/5-fluorouracil is associated with increased pathologic complete response and improved survival compared to carboplatin/paclitaxel in patients with locally advanced esophageal cancer," *Diseases of the Esophagus*, vol. 30, no. 7, pp. 1–7, 2017.
- [27] I. Y. H. Wong, K. O. Lam, R. Q. Zhang et al., "Neoadjuvant chemoradiotherapy using cisplatin and 5-fluorouracil (PF) versus carboplatin and paclitaxel (CROSS regimen) for esophageal squamous cell carcinoma (ESCC)," *Annals of Surgery*, vol. 272, no. 5, pp. 779–785, 2020.
- [28] M. A. Eloubeidi, R. Desmond, M. R. Arguedas, C. E. Reed, and C. M. Wilcox, "Prognostic factors for the survival of patients with esophageal carcinoma in the US," *Cancer*, vol. 95, no. 7, pp. 1434–1443, 2002.